Unbiased profiling of the human proinsulin biosynthetic interaction network reveals a role for peroxiredoxin 4 in proinsulin folding

Short running title: Human proinsulin biosynthetic interaction network

Authors: Duc T. Tran*[1], Anita Pottekat*[3,10], Saiful A. Mir[1,9], Salvatore Loguercio[4], Insook Jang[3], Alexandre Rosa Campos[8], Kathleen M. Scully[1], Reyhaneh Lahmy[1,11], Ming Liu[6,7], Peter Arvan[6], William E. Balch[4,5], Randal J. Kaufman[3§], Pamela Itkin-Ansari[1,2§]

*** These authors contributed equally to this work**

[1] Development, Aging and Regeneration program, Sanford Burnham Prebys Medical Discovery Institute, La Jolla, USA
[2] Department of Pediatrics, University of California, San Diego, La Jolla, CA, USA
[3] Degenerative Diseases Program, Sanford Burnham Prebys Medical Discovery Institute, La Jolla, USA
[4] The Scripps Research Institute, Department of Molecular Medicine, La Jolla, CA, USA
[5] Integrative Structural and Computational Biology, The Scripps Research Institute, La Jolla, CA, USA
[6] Division of Metabolism, Endocrinology & Diabetes, University of Michigan Medical School, Ann Arbor, USA
[7] Department of Endocrinology and Metabolism, Tianjin Medical University, Tianjin, China
[8] Sanford Burnham Prebys Medical Discovery Institute Proteomic Core, La Jolla, CA, USA
[9] Current address- Dept. of Zoology, City College, University of Calcutta, Kolkata, India
[10] Current address- Illumina, San Diego, CA, USA
[11] Current address- OncoMed Pharmaceuticals, Inc, Redwood City, CA, USA

§Corresponding authors

Pamela Itkin-Ansari, PhD

Adjunct Associate Professor
Sanford Burnham Prebys Medical Discovery Institute
Joint appointment-UCSD
Tel: 858-646-3100 x 3428
Email: pitkin@sbpdiscovery.org

Randal J Kaufman

Director and Professor Degenerative Diseases Program
Endowed Chair of Cell Biology
Sanford Burnham Prebys Medical Discovery Institute
Tel: 858.795.5149
Email: rkaufman@sbpdiscovery.org

Abstract

The beta cell protein synthetic machinery is dedicated to the production of mature insulin, which requires the proper folding and trafficking of its precursor, proinsulin. The complete network of proteins that mediate proinsulin folding and advancement through the secretory pathway, however, remains poorly defined. Here we used affinity purification and mass spectrometry to identify for the first time, the proinsulin biosynthetic interaction network in human islets. Stringent analysis established a central node of proinsulin interactions with ER folding factors, including chaperones and oxidoreductases, that is remarkably conserved in both sexes and across three ethnicities. The ER-localized peroxiredoxin PRDX4 was identified as a prominent proinsulin interacting protein. In beta cells, gene silencing of PRDX4 rendered proinsulin susceptible to misfolding, particularly in response to oxidative stress, while exogenous PRDX4 improved proinsulin folding. Moreover, proinsulin misfolding induced by oxidative stress or high glucose was accompanied by sulfonylation of PRDX4, a modification known to inactivate peroxiredoxins. Notably, islets from patients with Type II diabetes (T2D) exhibited significantly higher levels of sulfonylated PRDX4 than islets from healthy individuals. In conclusion, we have generated the first reference map of the human proinsulin interactome to identify critical factors controlling insulin biosynthesis, beta cell function, and T2D.

Introduction

It is estimated that 422 million adults are living with diabetes globally (http://www.who.int/en/). Beta cell physiology is tightly linked to all forms of diabetes and thus a better understanding of beta cell function is necessary to combat this disease.

The majority of the beta cell's protein synthetic machinery is dedicated to insulin biosynthesis, beginning with translocation of preproinsulin from the cytoplasm into the endoplasmic reticulum (ER) (1). Following cleavage of the signal peptide, proinsulin folding in the ER results in a three-dimensional structure stabilized by three intramolecular disulfide bonds (1). Only properly folded proinsulin molecules can transit from the ER to the Golgi apparatus. In the Golgi, proinsulin encounters zinc, further assembles into hexamers, and is finally transported to immature secretory granules, where processing enzymes proteolytically cleave proinsulin to mature insulin (and C-peptide) for release in response to elevated blood glucose (1).

Every second, 6000 preproinsulin molecules per beta cell are delivered to the ER for folding assisted by chaperones, co-chaperones and oxidoreductases (2). The critical role of proper folding in proinsulin biosynthesis is exemplified by rare heterozygous mutations in proinsulin that prevent correct disulfide bond formation (1). The misfolded proinsulin molecules resulting from a single mutant allele act in a dominant negative fashion to entrap wild-type proinsulin in the ER, causing Mutant *INS*-gene-induced Diabetes of Youth (MIDY) in both humans and animal models (1).

Type I and Type II diabetes (T1D and T2D) are typically associated with inflammation or oxidative stress, which may contribute to proinsulin misfolding and thereby limit the size of the properly-folded proinsulin population (1; 3). Moreover, we recently showed that even in healthy human islets, a portion of proinsulin is misfolded, suggesting that beta cells function near the limit of their capacity to produce properly folded proinsulin (3).

Misfolded proinsulin activates the unfolded protein response (UPR) signaled through two protein kinases, PERK and IRE1, and the transcription factor ATF6 (4) to help maintain cell proteostasis (5; 6). The chaperone BiP (HSPA5) is both a target and an essential regulator of the UPR. Early in progression to diabetes, the three branches of the UPR adapt the beta cell's ER to prevent further accumulation of misfolded proinsulin. This is accomplished by (i) attenuating proinsulin synthesis, (ii) inducing expression of genes that promote translocation, folding and trafficking in the ER and/or, (iii) activating genes that are involved in elimination of misfolded proinsulin through Endoplasmic Reticulum Associated Protein Degradation (ERAD) (4). Studies demonstrate that UPR signaling is essential to preserve beta cell function and survival, and if the UPR fails to restore proper proinsulin folding, beta cells undergo apoptosis (7; 8).

We recently showed that proinsulin misfolding in human islets is exacerbated by inhibition of the UPR factors PERK or of BiP (3), further highlighting the delicate nature of beta cell homeostasis. Indeed, defects anywhere in the biosynthetic network (folding, processing, trafficking, and exocytosis) can also lead to fulminant beta cell failure (9; 10). Therefore, it is critical to understand the cellular components that promote human beta cell insulin homeostasis and how they are maintained in the presence of extracellular insults (11). Proteomic analyses have catalogued the proteins in human islets (12-15), but these global analyses do not distinguish which proteins reside in beta cells, nor do they define the proteins that physically interact with proinsulin to direct its folding and maturation.

Here, we employed an unbiased affinity purification mass spectrometry (AP-MS) approach to identify the central machinery responsible for proinsulin production in human beta cells. The data reveal a rich proinsulin biosynthetic network that is remarkably conserved across a diverse group of donors. Further investigation of the network highlights a functional role for PRDX4 in promoting proinsulin folding that, importantly, may contribute to protection against T2D. Thus, the AP-MS data provide a roadmap for functional dissection of the proinsulin biosynthetic network and its impact on beta cell health.

Methods

Cell Culture

Human islets were cultured in Prodo Islet Complete Media (5.8 mM glucose, Prodo labs). MIN6 cells were cultured in DMEM with 4.5g/L glucose and L-glutamine, 0.34% Sodium bicarbonate, 1X penicillin, streptomycin, 275 nM β-mercaptoethanol (BME), 15% FBS. HEK 293A and 293T cells were cultured in DMEM with 4.5g/L glucose and L-glutamine, sodium pyruvate, 1X penicillin, streptomycin, 10% FBS.

Proinsulin Affinity purification - mass spectrometry (AP-MS)

Twenty-five hundred normal human islet Equivalents (IEQ) islets were lysed in 50 mM Tris pH 7.4, 150 mM NaCl and 1% TX-100, and 1X protease inhibitor cocktail (Thermofisher) were precleared with Protein G agarose beads, then immunoprecipitated with beads crosslinked to mouse IgG or proinsulin antibody (20G11) overnight at 4°C. A sample of beads was removed for Western blot and the majority of beads were processed for 2D LC-MS/MS analysis.

Immunoprecipitated proteins were subjected to denaturation in 8 M Urea in 50 mM ammonium bicarbonate buffer, reduced with tris (2-carboxyethyl)phosphine (TCEP), and alkylated with iodoacetamide (IAA). Urea concentration was diluted to 1 M using 50 mM ammonium bicarbonate and samples were digested overnight with mass spec grade Trypsin/Lys-C mix (Promega, Madison, WI). Digested proteins were finally desalted using a C18 TopTip (PolyLC, Columbia, MD) before subjecting to LC-MS/MS analysis. To label samples with TMT TMTsixplex™ Isobaric Label kit (ThermoFisher Scientific) was used according to manufacturer's protocol.

Samples were analyzed by 2DLC-MS/MS using a 2D nanoACQUITY Ultra Performance Liquid Chromatography (UPLC) system (Waters Corp., Milford, MA) coupled to an Orbitrap Velos Pro mass spectrometer (Thermo Fisher Scientific). Peptides were loaded onto the first dimension column, XBridge BEH130 C18 NanoEase (300 µm x 50 mm, 5 µm) equilibrated with solvent A (20 mM ammonium formate pH 10) at 2 µL/min. The first fraction was eluted from the first dimension column at 17% of solvent B (100% acetonitrile) for 4 min and transferred to the second dimension Symmetry C18 trap column 0.180 x 20 mm (Waters Corp., Milford, MA) using a 1:10 dilution with 99.9% second dimensional pump solvent A (0.1% formic acid in water) at 20 µL/min. Peptides were then eluted from the trap column and resolved on the analytical C18 BEH130 PicoChip column 0.075 x 100 mm, 1.7 µm particles (New Objective, MA) at low pH by increasing the composition of solvent B (100% acetonitrile) from 2 to 26% over 94 min at 400 nL/min. Subsequent fractions from the first dimension fractions were eluted at 19.5, 22, 26, and 65% solvent B and analyzed in similar manner. The mass spectrometer was operated in positive data-dependent acquisition mode with up to 5 MS2 spectra per duty cycle were triggered.

MS/MS spectra were searched against the Homo sapiens Uniprot protein sequence database (version January 2015) using Maxquant (version 1.5.5.1) with false discovery rate (FDR) set to 1%. (Note proinsulin was searched as insulin). Label free intensity was normalized by (Loess-R) with Normalyzer (16). MSStats was used to calculate a confidence (p-value) and fold change of Proinsulin IP/Control IgG IP for each protein (17). All data including *.raw data file, MaxQuant *.txt search results are available online at ProteomeXchange - Dataset ID PXD014476 (http://proteomecentral.proteomexchange.org/cgi/GetDataset).

Human islet lysates were similarly immunoprecipitated for proinsulin for validation studies. Bound proteins were eluted with 2X Laemmi buffer prior to Western blot analysis. MYC tagged proinsulin and FLAG tagged PRDX4 in HEK cells were immunoprecipitated using with anti-MYC, and anti-FLAG magnetic beads according to manufacturer protocol (Pierce).

Transfection

Plasmid expressing human PRDX4-FLAG was purchased from Sino Biological Inc. Vectors expressing WT or Akita mutant MYC- tagged human Proinsulin were generated in the Arvan lab (18). WT-PRDX4 pCDNA3.1 and C245A pCDNA 3.1 were a kind gift from Dr. Bulleid (19). pCDNA3.1 or GFP-PGK vectors were used as controls. Equal amounts of total DNA were transfected using Viafect (Promega) or Lipofectamine (Thermofisher) transfection reagent following manufacturer instructions.

Western blotting

Samples were prepared in 2X Laemmli sample buffer without (non-reducing) or with 2.5% BME (reducing), boiled (100^{o}C, 10 minutes), analyzed by SDS-PAGE and transferred to nitrocellulose membranes. Membranes were blocked and incubated with corresponding primary antibodies (4^{o}C, ON): Rabbit BiP (for human islets), Rabbit GRP94 (Cell Signaling Tech), or Rabbit ERDJ5, Rabbit Myo18A (ProteinTech), Goat PRDX4 (R&D System), Rabbit PRDX4 directly conjugated to Horse Radish Peroxidase (PRDX4-HRP, LSBio), Mouse 20G11 (generated in house), Rabbit PRDX-SO_3, and MYC-tag (Abcam); for mouse beta cells, Rabbit vinculin (Proteintech), Mouse proinsulin (HyTest Ltd.), Mouse insulin antibody (a kind gift from Dr Arvan), and Rabbit BiP (a kind gift from Dr Hendershot); for secondary antibodies, Goat anti-mouse, Goat anti-rabbit, Donkey anti goat and Donkey anti-guinea pig antibodies were used in 1:5000 (Li-Cor, IRDye®-800CW or IRDye®-680RD). Signals were visualized with Licor Odyssey CLX and western blot images were quantified by ImageJ. A detailed antibody list is in **Table S1**.

PRDX4 knockdown

Virus from retroviral vectors expressing GFP and shRNA targeting murine PRDX4 (Origene, Rockville, MD) or non-specific (NS) scramble control were used to infect MIN6 cells. Infected cells were selected by FACs sorting for high GFP intensity.

qPCR analysis

RNA was extracted using RNeasy kit (QIAGEN); and cDNAs were prepared using qScript cDNA SuperMix (Quantabio). qPCR was performed with SYBR Green I analyzed a LightCycler 96 (Roche). Each gene was normalized to 18S. Primers: 18S (CCA GAGCGAAAGCATTTGCCAAGA/TCGGCATCGTTTATGGTCGGAACT), XBP1-T (AAG AACACGCTTGGGAATGG/ACTCCCCTTGGCCTCCAC), XBP1-S (GAGTCCGCAGGTG/ GTGTCAGAGTCCATGGGA), PRDX4 (ACCAAGTATTTCCCACGATAGTC/GATCACTCC CTGCATCTAAGC).

Glucose stimulated insulin secretion (GSIS)

GSIS was measured using Mouse insulin and ultra-sensitive human insulin ELISA kits (Mercodia) according to manufacture recommendations.

Data and Resource Availability

The datasets generated and analyzed in the current study are available in the ProteomeXchange repository Dataset ID PXD014476, (http://proteomecentral.proteomexchange.org/cgi/GetDataset) and at NDEx (https://public.ndexbio.org/#/network/0c0a451c-88b1-11ea-aaef-0ac135e8bacf).

Results

Defining the Human Proinsulin Biosynthetic Interaction Network.

To identify the physical interactions that dictate proper proinsulin biosynthesis we first generated a series of monoclonal antibodies to human proinsulin. We chose a conformation specific monoclonal antibody that selectively recognizes human proinsulin by immunoprecipitation (IP) (20G11) in the presence of 1% Triton X-100, with negligible cross-reactivity to mature insulin (**Fig. S1A**). Because we recently found that even healthy islets harbor a subset of proinsulin molecules that are misfolded, we tested whether 20G11 recognizes misfolded human proinsulin in addition to the properly folded proinsulin. COS1 cells were transfected with wild-type human proinsulin or proinsulin variants bearing point mutations which cause severe misfolding leading to Mutant *INS*-gene-induced Diabetes of Youth (MIDY) (20). 20G11 efficiently immunoprecipitated WT as well as all MIDY proinsulin mutants tested (**Fig. S1B**). Therefore, we affinity purified proinsulin from human islets using 20G11 or control mouse IgG for Mass Spectrometry (AP-MS). Notably, IP of proinsulin provided beta-cell specificity in the context of intact islets, avoiding the need for islet dispersal or beta cell purification methods that can stress beta cells.

Initially, two MS quantification methodologies were compared; Label Free (LF) and Tandem Mass Tag (TMT) isobaric labeling approaches (**Fig. S2**). Numerous interactors were similarly identified with both methods, but the dynamic range of fold-change Proinsulin IP versus IgG IP detected by TMT was compressed, relative to LF as described by others (21). Therefore, LF was used for subsequent studies.

With the goal of identifying highly conserved proinsulin interactions at the core of normal human beta cell function, we procured islet preparations from 6 donors that included Caucasian, Hispanic and African American ethnicities as well as both sexes. The donors had no history of diabetes, BMI ranging from 21 to 25.4 and normal HbAIC (4.8%-5.5%) at the time of death (**Fig. 1A**). Equal numbers of islet equivalents were lysed and IP'ed with either 20G11 or mouse IgG conjugated beads and subjected to on-bead denaturation, reduction and trypsin digestion prior to LC-MS/MS analyses.

MS/MS spectra were searched against the Human Uniprot database and analyzed with MaxQuant. For statistical analyses, MSStats (17) was utilized to calculate a confidence score (*p*-value) for each protein based on the reproducibility of detection across samples. Comparison of MS/MS counts for proinsulin (bait) across the 6 islet samples revealed remarkable consistency in the recovery of proinsulin, suggesting little biological or technical variability (**Fig. 1B**). Similarly, the profile of prey proteins co-precipitated with proinsulin (FDR <1%) was highly consistent across the samples (**Fig. 1C**).

To identify the most robust proinsulin interactions for network analysis, the data were stringently filtered using the following criteria: (i) proinsulin IP/control IgG IP intensity ratios $\geq$ 2-fold ($\log_2 FC \geq 1$), (ii) $p \leq 0.05$, and (iii) total MS/MS across six samples ≥ 10. Moreover, to be certain that identified interactors were derived from beta cells, proteins were removed from analysis if their average mRNA expression in beta cells did not reach a minimum threshold of 1 CPM (counts per million) as reported in a recent single cell RNAseq study in human islets (22). The resulting dataset identified 461 proteins. These interactors were assigned to subcellular compartment or function, e.g. ER, using Protein Atlas as the primary source for classification as well as manual curation (23) (**Table S2** and ProteomeXchange ID PXD014476). For visualization of the network, nuclear, mitochondrial, and "undetermined" proteins were removed as described in reference (24). Thus, we constructed the first human proinsulin biosynthetic network (**Fig. 1D**). Increasing icon size represents significance (i.e. decreasing *p* value) and a thin line connects proinsulin to each interactor. Previously reported interactions among our identified proteins are depicted by gray lines with line thickness representing reported confidence score (25). An interactive map of Fig. 1D is also available: (https://public.ndexbio.org/#/network/0c0a451c-88b1-11ea-aaef-0ac135e8bacf).

Known proinsulin interactors spanning the entire proinsulin biosynthetic pathway were identified, beginning with ribosomal proteins and the SEC61B translocon that transfers nascent proinsulin from the cytosol into the ER. At the distal end of the secretory pathway we identified the proteolytic enzyme, PCSK1 (Prohormone Convertase 1), that cleaves the C-peptide/B chain junction of proinsulin. Given that enzyme interactions can be fleeting, identifying the proinsulin:PCSK1 association with high confidence ($p = 4.6 \times 10^{-5}$), demonstrates the sensitivity of the data. Conversely, the specificity of the affinity purification is highlighted by the absence of Islet Amyloid Polypeptide (IAPP), a highly expressed beta-cell protein that is stored and co-secreted with insulin, but is not thought to interact physically with proinsulin in normal islets (26).

Among the novel proinsulin interactors we identified was the unconventional Myosin-XVIIIa (MYO18A, $p=5.86 \times 10^{-6}$, $\log_2$FC Proinsulin IP/IgG IP= 3.71), validated in **Fig. S3A**. MYO18A links Golgi membranes to the cytoskeleton, likely participating in the tensile force required for vesicle budding from the Golgi (27). Therefore, our finding that MYO18A interacts with proinsulin, even if indirectly, supports the idea that there is specific recruitment of proinsulin (that withstands 1% Triton X-100) at the luminal aspect of budding Golgi membranes, as previously suggested (28).

ER localized folding factors that interact with proinsulin

To identify the signaling pathways at the core of the dataset we applied Ingenuity Pathway Analysis (IPA) (**Fig. 2A**). “Unfolded Protein Response”, the most enriched pathway, and related categories, e.g. “EIF2 signaling”, were comprised mainly of chaperones and co-chaperones. Signaling pathways that initially appeared as unusual, e.g. “Aldosterone”, were in fact also composed of these factors (29). To capture ER folding factors that may interact transiently or only with a misfolded subset of the larger population of proinsulin molecules, stringency was relaxed, using $p \leq 0.05$ and beta cell expression criteria **(Table S3)**. The identified ER folding factor subnetwork is shown in **Fig. 2B** where icon size represents $\log_2$FC proinsulin IP/control IgG IP and line thickness represents increasing significance (i.e. decreasing *p* value).

Among the ER localized interactors were proteins we previously showed play essential roles in proinsulin folding or beta cell health e.g. BiP/HSPA5, GRP94/HSP90B1 ERDJ6 (DNAJC3; p58^{IPK}) and PDIA1/P4HB, (3; 30-32) and novel factors like Quiescin Sulfhydryl Oxidase 1 QSOX1, an enzyme with no previously known substrates (33). The most robust proinsulin interaction (Log_2FC proinsulin IP/IgG IP 6.17, p=4.92x10^{-11}) was with Thioredoxin-Dependent Peroxiredoxin-4 (PRDX4) a 2-cysteine peroxiredoxin that utilizes luminal H_2O_2 to oxidize proteins (**Figs. 2B**, **S3B**) (24). A recent single-cell RNAseq study determined the expression level of PRDX4 specifically in human beta cells, shown relative to the beta cell transcription factor PDX1 and insulin in **Fig. S4** (34).

Functional characterization of PRDX4 suggests a role in proper proinsulin folding

PRDX4 peroxidase activity relies on a peroxidatic cysteine residue oxidized by luminal H_2O_2 to sulfenic acid which then forms a disulfide bond with the resolving cysteine on an adjacent PRDX4 molecule. Thus, PRDX4 enzymatic activity requires dimerization or higher order structures (24). To investigate the conformational composition of PRDX4 in islets, we used nonreducing SDS-PAGE of murine islets. Virtually all PRDX4 protein was found in disulfide linked dimers (at approximately 52 KDa) and high molecular weight (HMW) complexes, with only a small fraction as the 28 KDa monomer (**Fig. 2C, left lane**). Importantly, the HMW PRDX4 containing complexes clearly involve additional proteins as not all bands are multimers of 28 KDa. To validate the specificity of the PRDX4 complexes, live islets were treated with increasing concentrations of dithiothreitol (DTT, a reducing agent). High DTT conditions resolved HMW PRDX4 species to monomer and the particularly stable dimer 52KDa band (35) without affecting the overall PRDX4 expression or expression of proinsulin and insulin. The data indicate that the complexes specifically contain PRDX4 and suggest that PRDX4 interactions with additional proteins occur via disulfide bonds.

To determine whether PRDX4 interacts with both WT and misfolded proinsulin, HEK293 cells were co-transfected with plasmids expressing human PRDX4 and either WT or MIDY *Akita* mutant human proinsulin. The *Akita* mutation in the cysteine at A7 (C(A7)Y) leaves the B7 cysteine without its disulfide pairing partner required for proinsulin folding (1). Immunoprecipitation of WT or Akita proinsulin co-precipitated PRDX4, revealing that PRDX4 interacts with both folded and misfolded proinsulin (**Fig. S3C**). Conversely, PRDX4 immunoprecipitation from similarly prepared samples co-IP'ed both WT and Akita proinsulin (**Fig. S3C**).

Given the importance of BiP to proinsulin folding, we asked whether proinsulin:PRDX4 interactions required BiP. HEK cells transfected with PRDX4 and human proinsulin were treated with the BiP ATPase inhibitor HA15, the Shiga-toxic *E. coli* virulence factor SubAB that cleaves and inactivates BiP (36), or mutant SubAB, an enzymatically inactive form of SubAB (**Fig 3A**). Immunoprecipitation of PRDX4 co-IP'ed proinsulin independent of BiP inhibition or cleavage, indicating that intact or enzymatically active BiP is not required for proinsulin:PRDX4 interactions (**Fig 3A**). These experiments further revealed that PRDX4 interacts physically with BiP in both the presence and absence of proinsulin (**Fig 3B**). Controls showed that all PRDX4 conformations were immunoprecipitated and that proinsulin and BiP did not bind to beads non-specifically (**Fig**. **S5A,B**). Thus, PRDX4 binds to proinsulin independent of BiP and PRDX4 binds to BiP independent of proinsulin.

To determine whether proinsulin folding is assisted by PRDX4, lentiviral vectors expressing shRNA were used to deplete PRDX4 in MIN6 cells, achieving 64 – 75% PRDX4 knockdown compared to controls (**Fig. 4A,B**). PRDX4 knockdown triggered modest proinsulin misfolding as revealed by an increase of HMW complexes. Moreover, PRDX4-depleted MIN6 cells were hypersensitive to proinsulin misfolding induced by oxidant challenge with 100 µM Menadione (30) or 1 mM H_2O_2 for 1 hour (**Fig. 4A**). We similarly observed that Menadione induced oxidative stress caused proinsulin misfolding in human islets (**Fig. S6**). Of note, proinsulin misfolding was accompanied by conformational changes of PRDX4 into HMW disulfide bonded complexes, suggesting that PRDX4 may be recruited to client proteins during oxidative stress.

We considered that decreased PRDX4 expression might activate the UPR. mRNA expression levels of the factors BiP, PDIA1, and CHOP were not altered by low PRDX4 expression (not shown). We found however that reduced expression of PRDX4 decreased the ratio of the IRE1 target spliced X-box binding protein-1 (37). (XBP1s) mRNA, relative to total XBP-1 (XBP1s/XBP1t), which was surprising, warranting further investigation of UPR (**Fig. 4B**).

We next asked whether increased expression of PRDX4 could promote proper proinsulin folding. HEK293 cells were co-transfected WT human proinsulin and either control plasmid, WT PRDX4, or a mutant form of PRDX4 (C245A) that lacks enzymatic activity (19) (**Fig. 4C**). Exogenous WT PRDX4 decreased HMW proinsulin species (>28kD) relative to controls, while the C245A mutant PRDX4 did not (**Fig. 4C**), suggesting that PRDX4 oxidoreductase activity is required to promote proinsulin folding. Both WT and mutant PRDX4 induced BiP expression but the finding that only WT PRDX4 promoted proinsulin folding indicates that BiP upregulation alone was not responsible for improved proinsulin folding by WT PRDX4.

The expression of multiple ER proteins increases in response to glucose stimulation of beta cells (37); we therefore probed whether PRDX4 expression was glucose responsive. (**Fig. 5A**). In MIN6 cells high glucose treatment overnight resulted in a 3.3-fold increase in secreted insulin, accompanied by a 73% increase in intracellular steady state levels of proinsulin but no change in PRDX4 expression (**Fig. 5A**). Non-reducing SDS-PAGE analysis of proinsulin showed that the ratio of misfolded to properly folded remained constant in high glucose conditions.

Under high H_2O_2 conditions the peroxidactic cysteine of PRDX4 can become irreversibly overoxidized to sulfonic acid (PRDX4-SO_3, referred to as sulfonylation) that inactivates PRDX4 enzymatic activity (38). We therefore investigated the effect of high glucose on PRDX4 sulfonylation in MIN6 cells, finding that high glucose significantly increased sulfonylated PRDX4 relative to total PRDX4 (**Fig. 5A**).

We next examined the effects of high glucose on proinsulin folding and PRDX4 in human islets. Similar to MIN6 cells, high glucose stimulated insulin release into the media (**Fig. 5B**), a significant increase in the steady state level of intracellular proinsulin, and no change in PRDX4 expression. In human islets, glucose induced a 2.3-fold increase in BiP in response to glucose. Notably, non-reducing SDS-PAGE revealed that high glucose increased the fraction of proinsulin that was misfolded in human islets (**Fig. 5B**). In contrast to MIN6 cells, normal human islets treated overnight with high glucose did not exhibit PRDX4 sulfonylation.

We considered that the difference in PRDX4 status between MIN6 and human islets might be due to normoglycemic *in vivo* conditions for the human islets versus long term culture of MIN6 cells in high glucose media. This prompted us ask whether chronic high glucose in human T2D might induce PRDX4 sulfonylation. Indeed, examination of a series of human islet samples from patients with T2D (n=4, HbA1C 6.5 - 8.5 % or 48 - 69 mmol/mol) versus healthy individuals (n=4, HbA1C 4.2 - 5.9 or 22 – 41 mmol/mol) revealed for the first time that the fraction of sulfonylated PRDX4 in islets is elevated in T2D (3.3-fold, *p*=0.011) (**Fig 6**). Thus, PRDX4 appears to be selectively inactivated in islets from patients with T2D.

Discussion

Here we provide the first reference map of human proinsulin's transit through the biosynthetic pathway. The most striking feature of this dataset is the tight conservation of the human proinsulin biosynthetic network across 6 donors reflecting 3 ethnicities and both sexes. A technical aspect that may have contributed to the data concordance was that human islets for AP-

MS were procured from a single source to avoid artifacts resulting from site-specific islet isolation practices. We corroborate previously identified proinsulin interacting proteins, (8; 30; 31) and extend those studies to provide an entire interaction network.

We previously performed AP-MS to identify proinsulin and insulin interactors in murine MIN6 cells (39). Consistent with those studies, here we identified ERDJ3, DNAJC3/p58^{IPK}, and ERP44 as high confidence human proinsulin interacting proteins. Not surprisingly, TMEM24, which interacted more robustly with mature insulin than with proinsulin in MIN6 cells, was not identified in this study focused solely on proinsulin interactions in human islets.

Among the most significant newly identified proinsulin interacting proteins was PRDX4. It will be of interest to determine whether the proinsulin:PRDX4 interaction is direct and the other potential members of the complex. One of these factors may well be BiP, that we showed binds to both proinsulin and PRDX4. It has also been suggested that clients of PRDX4 are PDI family members, e.g. PDIA1 that was also identified in our study (40).

In yeast, it was suggested that the single PRDX-like protein is a molecular triage agent that absorbs oxidation (41). PRDX4 is not essential for survival in mice (42), but we find that proinsulin is more prone to misfolding when PRDX4 levels are low, particularly in cells stressed by oxidant treatment. The idea that PRDX4 becomes may be required under stress conditions is consistent with findings that mice lacking PRDX4 are more prone to LPS induced toxicity (43) or to dextran sulfate sodium-induced colitis (44). Further, in MEFs under normal conditions, loss of the oxidoreductase ERO1 (a proinsulin interactor identified here) renders the cells dependent on PRDX4 for growth (24) and in mouse hearts, loss of the oxidoreductase QSOX1, another of our identified proinsulin interactors, induces compensatory upregulation of PRDX4 (45). Together, our data and the work of others suggest that PRDX4 function may be redundant with other oxidoreductases under normal conditions but become critical under stress. Whether PRDX4 is required to buffer diabetogenic islet stress *in vivo* is an avenue for further investigation.

We show that overexpression of PRDX4 improves proinsulin folding. In accordance with this finding, others have observed that increased PRDX4 expression in INS1 cells improved glucose-induced insulin secretion (46) and in mice, overexpression of PRDX4 provided protection against streptozotocin-induced diabetes (47).

Excessive oxidation inactivates PRDX4 by sulfonylation, a two-step process. PRDX4 sulfenic acid is first modified to sulfinic acid, which may be the rate limiting step. Further oxidation then results in irreversible sulfonylation (38). Acute high glucose treatment induced PRDX4 sulfonylation in MIN6 cells, similar to a report in INS-1 cells (46), but not in human islets. We hypothesize that chronic exposure of the MIN6 and INS-1 cells to high glucose culture media may shift PRDX4 from sulfenic acid to sulfinic acid, poising PRDX4 for sulfonylation in those cells. In contrast, the human islets were procured from normoglycemic donors where sulfenic acid may be the predominant form of PRDX4.

The idea that chronic high glucose predisposes PRDX4 to sulfonylation is consistent with our data showing increased PRDX4 sulfonylation in islets from patients with T2D. Notably, the proinsulin from these samples also exhibited a trend toward increased misfolding. Together, the data suggest that beta cells in patients with T2D have increased oxidative stress and/or diminished capacity to handle oxidative stress, which is in agreement with previous studies (48; 49). PRDX4-SO_3 may in fact be a measure of the degree of oxidative stress beta cells. PRDX4 can also be secreted and has been identified in extracellular vesicles (43). It is intriguing that serum samples from patients with T2D have higher levels of circulating PRDX4 than controls

(50). It is not yet known whether the circulating PRDX4 emanates from beta cells and/or whether the PRDX4 is modified by sulfonylation, questions with implications for diagnosing beta cell stress in a minimally invasive manner.

In summary, we have identified a complex network of factors that dictate proinsulin folding and trafficking through the exocytic pathway in human beta cells. The proinsulin interaction network provides a critical resource to characterize previously unknown molecular features of the beta cell secretory pathway and to determine their relevance in diabetes.

Acknowledgment

We thank Dr. Philip Rosenstiel for helpful discussion. Human pancreatic islets were procured from PRODO labs and from the NIDDK-funded Integrated Islet Distribution Program (IIDP) at City of Hope, NIH Grant #2UC4DK098085 and the JDRF-funded IIDP Islet Award Initiative. The SubAB was a kind gift from Drs. Adrienne W and James C Paton. We thank the Proteomics, Virology, and Bioinformatic Core facilities at SBPMDI.

Funding

This work was supported by NIH R24 DK110973 (P I-A, PA and RJK), and JDRF research grant 2-SRA-2015-47-M-R (P I-A, RJK, WEB).

Author contributions

P.I.-A., R.J.K., W.E.B., P.A., conceived and designed the study and M.L contributed to the study design. W.E.B. provided the 20G11 antibody. A.P. and R.L. performed the affinity purification-mass spectrometry experiment in human islets. A.R.C. performed mass spectrometry data acquisition. D.T.T., S.L., A.R.C. performed statistical and bioinformatic analysis of mass spectrometry data. D.T.T. and S.A.M. validated potential interactors in human islets, performed PRDX4 functional studies and data analysis. I.J. performed murine islet studies on PRDX4. D.T.T., P.I.-A. prepared tables and figures. P.I.-A., D.T.T. and K.M.S., R.J.K. and P.A. wrote the manuscript.

Conflict of Interest

All authors report that they do not have a conflict of interest.

Guarantor statement

P.I.-A. *is the guarantor of this work and, as such, had full access to all the data in the study and takes responsibility for the integrity of the data and the accuracy of the data analysis.*

REFERENCES:

1. Liu M, Weiss MA, Arunagiri A, Yong J, Rege N, Sun J, Haataja L, Kaufman RJ, Arvan P: Biosynthesis, structure, and folding of the insulin precursor protein. Diabetes, Obesity and Metabolism 2018;20:28-50
2. Schuit FC, Kiekens R, Pipeleers DG: Measuring the balance between insulin synthesis and insulin release. Biochemical and biophysical research communications 1991;178:1182-1187
3. Arunagiri A, Haataja L, Pottekat A, Pamenan F, Kim S, Zeltser LM, Paton AW, Paton JC, Tsai B, Itkin-Ansari P: Proinsulin misfolding is an early event in the progression to type 2 diabetes. eLife 2019;8:e44532
4. Scheuner D, Kaufman RJ: The unfolded protein response: a pathway that links insulin demand with β-cell failure and diabetes. Endocrine reviews 2008;29:317-333
5. Hutt DM, Balch WE: Expanding proteostasis by membrane trafficking networks. Cold Spring Harbor perspectives in biology 2013;5:a013383
6. Powers ET, Balch WE: Diversity in the origins of proteostasis networks—a driver for protein function in evolution. Nature reviews Molecular cell biology 2013;14:237
7. Wu J, Kaufman R: From acute ER stress to physiological roles of the unfolded protein response. Cell death and differentiation 2006;13:374
8. Scheuner D, Vander Mierde D, Song B, Flamez D, Creemers JW, Tsukamoto K, Ribick M, Schuit FC, Kaufman RJ: Control of mRNA translation preserves endoplasmic reticulum function in beta cells and maintains glucose homeostasis. Nature medicine 2005;11:757
9. Lu M, Lawrence DA, Marsters S, Acosta-Alvear D, Kimmig P, Mendez AS, Paton AW, Paton JC, Walter P, Ashkenazi A: Opposing unfolded-protein-response signals converge on death receptor 5 to control apoptosis. Science 2014;345:98-101
10. Roth DM, Hutt DM, Tong J, Bouchecareih M, Page L, Wang N, Seeley T, Dekkers JF, Beekman JM, Garza D, Miller J, Masliah E, Morimoto RI, Balch WE: Modulation of the maladaptive stress response to mange diseases of protein folding. PloS Biol 2014
11. Back SH, Kaufman RJ: Endoplasmic reticulum stress and type 2 diabetes. Annual review of biochemistry 2012;81:767-793
12. Waanders LF, Chwalek K, Monetti M, Kumar C, Lammert E, Mann M: Quantitative proteomic analysis of single pancreatic islets. Proceedings of the National Academy of Sciences 2009;106:18902-18907
13. Ahmed M, Forsberg J, Bergsten P: Protein profiling of human pancreatic islets by two-dimensional gel electrophoresis and mass spectrometry. Journal of proteome research 2005;4:931-940
14. Schrimpe-Rutledge AC, Fontes G, Gritsenko MA, Norbeck AD, Anderson DJ, Waters KM, Adkins JN, Smith RD, Poitout V, Metz TO: Discovery of novel glucose-regulated proteins in isolated human pancreatic islets using LC-MS/MS-based proteomics. Journal of proteome research 2012;11:3520-3532
15. Zhang L, Lanzoni G, Battarra M, Inverardi L, Zhang Q: Proteomic profiling of human islets collected from frozen pancreata using laser capture microdissection. Journal of proteomics 2017;150:149-159
16. Chawade A, Alexandersson E, Levander F: Normalyzer: a tool for rapid evaluation of normalization methods for omics data sets. Journal of proteome research 2014;13:3114-3120
17. Choi M, Chang C-Y, Clough T, Broudy D, Killeen T, MacLean B, Vitek O: MSstats: an R package for statistical analysis of quantitative mass spectrometry-based proteomic experiments. Bioinformatics 2014;30:2524-2526
18. Liu M, Haataja L, Wright J, Wickramasinghe NP, Hua Q-X, Phillips NF, Barbetti F, Weiss MA, Arvan P: Mutant INS-gene induced diabetes of youth: proinsulin cysteine residues impose dominant-negative inhibition on wild-type proinsulin transport. PloS one 2010;5:e13333
19. Tavender TJ, Sheppard AM, Bulleid NJ: Peroxiredoxin IV is an endoplasmic reticulum-localized enzyme forming oligomeric complexes in human cells. Biochemical Journal 2008;411:191-199
20. Liu M, Hodish I, Rhodes CJ, Arvan P: Proinsulin maturation, misfolding, and proteotoxicity. Proceedings of the National Academy of Sciences 2007;104:15841-15846

21. Megger DA, Pott LL, Ahrens M, Padden J, Bracht T, Kuhlmann K, Eisenacher M, Meyer HE, Sitek B: Comparison of label-free and label-based strategies for proteome analysis of hepatoma cell lines. Biochimica et Biophysica Acta (BBA)-Proteins and Proteomics 2014;1844:967-976
22. Wang YJ, Schug J, Won K-J, Liu C, Naji A, Avrahami D, Golson ML, Kaestner KH: Single-cell transcriptomics of the human endocrine pancreas. Diabetes 2016;65:3028-3038
23. Uhlén M, Fagerberg L, Hallström BM, Lindskog C, Oksvold P, Mardinoglu A, Sivertsson Å, Kampf C, Sjöstedt E, Asplund A: Tissue-based map of the human proteome. Science 2015;347:1260419
24. Zito E, Melo EP, Yang Y, Wahlander Å, Neubert TA, Ron D: Oxidative protein folding by an endoplasmic reticulum-localized peroxiredoxin. Molecular cell 2010;40:787-797
25. Alanis-Lobato G, Andrade-Navarro MA, Schaefer MH: HIPPIE v2. 0: enhancing meaningfulness and reliability of protein–protein interaction networks. Nucleic acids research 2016:gkw985
26. Knight JD, Williamson JA, Miranker AD: Interaction of membrane-bound islet amyloid polypeptide with soluble and crystalline insulin. Protein Science 2008;17:1850-1856
27. Taft MH, Behrmann E, Munske-Weidemann L-C, Thiel C, Raunser S, Manstein DJ: Functional characterization of human myosin-18A and its interaction with F-actin and GOLPH3. Journal of Biological Chemistry 2013;288:30029-30041
28. Orci L, Ravazzola M, Perrelet A: (Pro)insulin associates with Golgi membranes of pancreatic B cells. PNAS 1984;81:6743-6746
29. Braakman I, Bulleid NJ: Protein folding and modification in the mammalian endoplasmic reticulum. Annual review of biochemistry 2011;80:71-99
30. Jang I, Pottekat A, Poothong J, Yong J, Lagunas-Acosta J, Charbono A, Chen Z, Scheuner DL, Liu M, Itkin-Ansari P: PDIA1/P4HB is required for efficient proinsulin maturation and ß cell health in response to diet induced obesity. eLife 2019;8:e44528
31. Ghiasi SM, Dahlby T, Andersen CH, Haataja L, Petersen S, Omar-Hmeadi M, Yang M, Pihl C, Bresson SE, Khilji MS: Endoplasmic Reticulum Chaperone Glucose-Regulated Protein 94 Is Essential for Proinsulin Handling. Diabetes 2019;68:747-760
32. Han J, Song B, Kim J, Kodali VK, Pottekat A, Wang M, Hassler J, Wang S, Pennathur S, Back SH: Antioxidants complement the requirement for protein chaperone function to maintain β-cell function and glucose homeostasis. Diabetes 2015;64:2892-2904
33. Rudolf J, Pringle MA, Bulleid NJ: Proteolytic processing of QSOX1A ensures efficient secretion of a potent disulfide catalyst. Biochemical Journal 2013;454:181-190
34. Wang YJ, Schug J, Won KJ, Liu C, Naji A, Avrahami D, Golson ML, Kaestner KH: Single-Cell Transcriptomics of the Human Endocrine Pancreas. Diabetes 2016;65:3028-3038
35. Tavender TJ, Springate JJ, Bulleid NJ: Recycling of peroxiredoxin IV provides a novel pathway for disulphide formation in the endoplasmic reticulum. The EMBO journal 2010;29:4185-4197
36. Paton AW, Beddoe T, Thorpe CM, Whisstock JC, Wilce MC, Rossjohn J, Talbot UM, Paton JC: AB 5 subtilase cytotoxin inactivates the endoplasmic reticulum chaperone BiP. Nature 2006;443:548
37. Hassler JR, Scheuner DL, Wang S, Han J, Kodali VK, Li P, Nguyen J, George JS, Davis C, Wu SP: The IRE1α/XBP1s pathway is essential for the glucose response and protection of β cells. PLoS biology 2015;13:e1002277
38. Wood ZA, Schröder E, Robin Harris J, Poole LB: Structure, mechanism and regulation of peroxiredoxins. Trends in Biochemical Sciences 2003;28:32-40
39. Pottekat A, Becker S, Spencer KR, Yates III JR, Manning G, Itkin-Ansari P, Balch WE: Insulin biosynthetic interaction network component, TMEM24, facilitates insulin reserve pool release. Cell reports 2013;4:921-930
40. Zito E: PRDX4, an endoplasmic reticulum-localized peroxiredoxin at the crossroads between enzymatic oxidative protein folding and nonenzymatic protein oxidation. Antioxidants & redox signaling 2013;18:1666-1674
41. Day AM, Brown JD, Taylor SR, Rand JD, Morgan BA, Veal EA: Inactivation of a peroxiredoxin by hydrogen peroxide is critical for thioredoxin-mediated repair of oxidized proteins and cell survival. Molecular cell 2012;45:398-408

42. Iuchi Y, Okada F, Tsunoda S, Kibe N, Shirasawa N, Ikawa M, Okabe M, Ikeda Y, Fujii J: Peroxiredoxin 4 knockout results in elevated spermatogenic cell death via oxidative stress. Biochemical Journal 2009;419:149-158
43. Lipinski S, Pfeuffer S, Arnold P, Treitz C, Aden K, Ebsen H, Falk-Paulsen M, Gisch N, Fazio A, Kuiper J: Prdx4 limits caspase-1 activation and restricts inflammasome-mediated signaling by extracellular vesicles. The EMBO journal 2019;38
44. Takagi T, Homma T, Fujii J, Shirasawa N, Yoriki H, Hotta Y, Higashimura Y, Mizushima K, Hirai Y, Katada K: Elevated ER stress exacerbates dextran sulfate sodium-induced colitis in PRDX4-knockout mice. Free Radical Biology and Medicine 2019;134:153-164
45. Caillard A, Sadoune M, Cescau A, Meddour M, Gandon M, Polidano E, Delcayre C, Da Silva K, Manivet P, Gomez A-M: QSOX1, a novel actor of cardiac protection upon acute stress in mice. Journal of molecular and cellular cardiology 2018;119:75-86
46. Mehmeti I, Lortz S, Elsner M, Lenzen S: Peroxiredoxin 4 improves insulin biosynthesis and glucose-induced insulin secretion in insulin-secreting INS-1E cells. Journal of Biological Chemistry 2014;289:26904-26913
47. Ding Y, Yamada S, Wang K-Y, Shimajiri S, Guo X, Tanimoto A, Murata Y, Kitajima S, Watanabe T, Izumi H: Overexpression of peroxiredoxin 4 protects against high-dose streptozotocin-induced diabetes by suppressing oxidative stress and cytokines in transgenic mice. Antioxidants & redox signaling 2010;13:1477-1490
48. Lupi R, Del Guerra S, Mancarella R, Novelli M, Valgimigli L, Pedulli G, Paolini M, Soleti A, Filipponi F, Mosca F: Insulin secretion defects of human type 2 diabetic islets are corrected in vitro by a new reactive oxygen species scavenger. Diabetes & metabolism 2007;33:340-345
49. Ceriello A, Mercuri F, Quagliaro L, Assaloni R, Motz E, Tonutti L, Taboga C: Detection of nitrotyrosine in the diabetic plasma: evidence of oxidative stress. Diabetologia 2001;44:834-838
50. El Eter E, Al-Masri A: Peroxiredoxin isoforms are associated with cardiovascular risk factors in type 2 diabetes mellitus. Brazilian Journal of Medical and Biological Research 2015;48:465-469

Figure Legends

Figure 1- Defining the Proinsulin Biosynthetic Interaction Network. (A) Human islets from 6 donors with no history of diabetes and with normal HbA1C were used for final AP-MS studies. (B) Total MS/MS counts for proinsulin (bait) in the Proinsulin IP or IgG IP from the six islet preparations reported in (A). (C) Venn diagram showing shared and unique proinsulin interacting proteins identified with FDR $\leq$ 1% in the six islet preparations. (D) Network analysis of robust proinsulin protein:protein interactions generated by Cytoscape. Data were filtered using all of the following criteria: (i) Proinsulin IP/Control IP intensity ratios $\geq$ 2-fold, (ii) $p \leq 0.05$, (iii) total MS/MS across 6 samples ≥ 10, and (iv) mRNA expression in single cell mRNA profiling of beta cells of at least 1 CPM (counts per million) (34). Protein categories defined by Protein Atlas (23). Interacting proteins in the categories; nucleus, mitochondria, as well as those of undetermined category, are not visualized in this figure but are included in uploaded analysis. Increasing icon size depicts increasing significance. Gray lines depict previously reported protein:protein interactions and line thickness reflects confidence score (25).

Figure 2- Human proinsulin interacts with ER resident folding factors, including PRDX4. (A) Ingenuity Pathway Analysis (IPA) of identified proinsulin interactors (not included are mitochondrial and ribosomal proteins) reveals enrichment of Unfolded Protein Response as a major pathway involved in proinsulin biosynthesis. (B) Proinsulin interacting ER resident folding factors with *p* value ≤ 0.05. Icon size reflects $\log_2$FC proinsulin IP/IgG IP and line thickness represents increasing significance (decreasing *p* values). (C) PRDX4 conformational analysis in normal murine islets. Live islets treated with a gradient of DTT concentrations ranging from 1 to 15 mM for 20 minutes (or untreated control (0), left lane) were lysed and

resolved by non-reducing SDS-PAGE immunoblotted for PRDX4 and by reducing SDS-PAGE immunoblotted for PRDX4, proinsulin, insulin and vinculin. Intensity of disulfide linked HMW complex (size indicated 49 – 198 kDa) versus PRDX4 monomer (28 kDa) is quantified in graph. Molecular weight markers are shown.

Figure 3- PRDX4 interacts with proinsulin and BiP, independent of each other. (A) HEK293T cells were transfected with plasmids expressing human Proinsulin-MYC and human PRDX4-FLAG or untransfected. After 44 hours cells were treated with SubAb that cleaves BiP (Sub, 2 μg/mL, 4 hrs), Mutant SubAb as control (Msub, 2 μg/mL, 4 hrs), the BiP inhibitor HA15 (10 μM, 4 hrs) or untreated, followed by cell lysis and immunoprecipitation with anti-FLAG magnetic beads. 3% of Lysate (L) and 20% of immunoprecipitate (IP) were analyzed on reducing SDS-PAGE. Note, antibody light chain band appears just below PRDX4. (B) HEK293A cells were transfected with equal amounts of total plasmid in combination of control pCDNA (-), human Proinsulin-MYC and human PRDX4-FLAG. Resulting lysates were subject to immunoprecipitation with anti-FLAG magnetic beads. Lysates (L) and IP fractions were immunoblotted for BiP, PRDX4 or MYC tag (proinsulin). Red arrows identify BiP and blue arrow identifies Proinsulin-MYC band.

Figure 4- PRDX4 facilitates proinsulin folding. (A) Loss of PRDX4 increases proinsulin misfolding. PRDX4 was knocked down in MIN6 cells by stable expression of PRDX4 shRNA (PRDX4#1 and PRDX4#2) or scrambled non-specific shRNA (NS). Cells were untreated or treated with the oxidant menadione (Men) (100 μM, 1 hr) or H_2O_2 (1 mM, 1 hr). Non-reducing SDS-PAGE were immunoblotted with proinsulin antibody CCI17. Bottom panels of non-reducing gel shows darker exposure of proinsulin monomer band at approximately 6KDa. Reducing gels were immunoblotted for Vinculin, PRDX4, and total Proinsulin. Accompanying

graphs (right) show quantification of HMW proinsulin bands from 14 – 49 KDa or 49 – 198 KDa from non-reducing gel and total PRDX4 from reducing gel, normalized by Vinculin. The data are representative of 4 independent experiments. (B) mRNA derived from cells described in (A) confirms PRDX4 knockdown in MIN6 stably expressed PRDX4 shRNA by qPCR using 3 biological replicates per line. Lower panel: qPCR analysis of the ER stress marker 'spliced XBP1' relative to total XBP1 was under-represented in the PRDX4 knockdown. (C) HEK293T cells were transfected with equal amounts of plasmids containing combinations of human Proinsulin-MYC, human WT-PRDX4, human PRDX4 harboring a mutation in the resolving cysteine (C245A-PRDX4) and GFP, or untransfected. Resulting lysates were analyzed by non-reducing and reducing SDS-PAGE. Accompanying graph showed ratios of disulfide-bonded high molecular weight complexes (MW >28) over corresponding total proinsulin intensity determined on reducing gel. $^{**}p<0.01$.

Figure 5- Analysis of high glucose induced proinsulin misfolding and PRDX4 expression in MIN6 and human islets. (A) MIN6 cells were glucose starved for 1 hour and then treated with Low (2.2 mM, n=3) or High (22 mM, n=3) glucose [Glu] for 22.5 hours. HMW proinsulin complexes (red bar) were resolved on non-reducing SDS-PAGE. Samples were also analyzed on reducing SDS-PAGE and immunoblotted for BiP, total proinsulin, PRDX4, and PRDX-SO_3 along with loading controls (Vinculin and GAPDH). PRDX4 and PRDX-SO_3 were immunoblotted with two different primary and secondary antibodies on the same membrane and the images were merged. Red arrow shows PRDX4-SO_3 band identified by the PRDX-SO_3 antibody. Accompanying graphs show secreted (scr) insulin assayed by ELISA in the media relative to Vinculin in lysate (Lys), HMW proinsulin complexes in lysate (red bar) to Vinculin, HMW proinsulin complexes (red bar) in lysate to total proinsulin, BiP to Vinculin, total PRDX4

to Vinculin, and PRDX4-SO_3 band normalized to total PRDX4. (B) Human islets were glucose starved for 1 hour prior to treatment with Low (3 mM, n=4) or High (30 mM, n=4) glucose [Glu] for 18 hours. HMW proinsulin complexes (red bar) were resolved on non-reducing SDS-PAGE. Samples were analyzed on reducing and non-reducing SDS-PAGE as described in (A). Accompanying graphs are as described in A except that GAPDH is used to normalize secreted insulin, HMW proinsulin, and PRDX4 instead of vinculin.

Figure 6- T2D islets exhibit increased PRDX4 sulfonylation. (A) 8.55 µg of protein from human islet preparations from 4 normal individuals and 4 patients with Type 2 Diabetes (T2D) were analyzed by non-reducing SDS-PAGE (upper panel) and immunoblotted for proinsulin (one representative sample is displayed here). The accompanying graph shows quantification of HMW bands (size range indicated by curved bracket) normalized by proinsulin monomer on the non-reducing gel for all 8 samples. Reducing gels were immunoblotted for total proinsulin and GAPDH loading control (bottom panels). (B) All samples were immunoblotted for both PRDX4 (green) and sulfonylated PRDXs (i.e. PRDX-SO_3, red) on the same membrane. Merged image shows co-localization of PRDX4 band with its sulfonylated version at the same molecular weight. Intensity of the sulfonylated PRDX4 bands (yellow arrow) versus total PRDX4 were quantified.

Figure 1

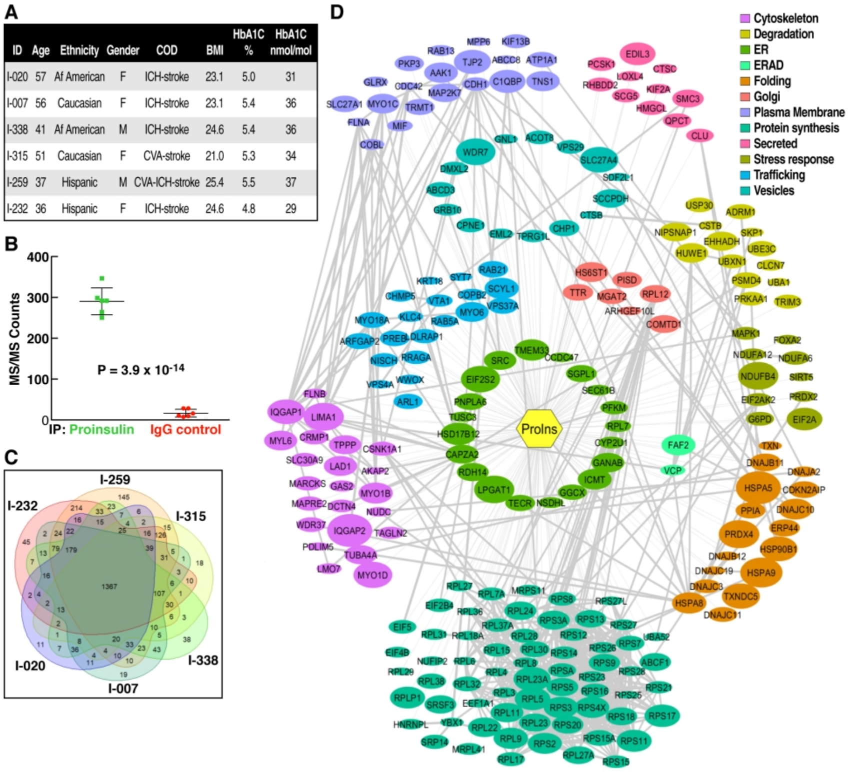

ID	Age	Ethnicity	Gender	COD	BMI	HbA1C %	HbA1C nmol/mol
I-020	57	Af American	F	ICH-stroke	23.1	5.0	31
I-007	56	Caucasian	F	ICH-stroke	23.1	5.4	36
I-338	41	Af American	M	ICH-stroke	24.6	5.4	36
I-315	51	Caucasian	F	CVA-stroke	21.0	5.3	34
I-259	37	Hispanic	M	CVA-ICH-stroke	25.4	5.5	37
I-232	36	Hispanic	F	ICH-stroke	24.6	4.8	29

Figure 1- Defining the Proinsulin Biosynthetic Interaction Network. (A) Human islets from 6 donors with no history of diabetes and with normal HbA1C were used for final AP-MS studies. (B) Total MS/MS counts for proinsulin (bait) in the Proinsulin IP or IgG IP from the six islet preparations reported in (A). (C) Venn diagram showing shared and unique proinsulin interacting proteins identified with FDR ≤ 1% in the six islet preparations. (D) Network analysis of robust proinsulin protein:protein interactions generated by Cytoscape. Data were filtered using all of the following criteria: (i) Proinsulin IP/Control IP intensity ratios ≥ 2-fold, (ii) p ≤0.05, (iii) total MS/MS across 6 samples ≥10, and (iv) mRNA expression in single cell mRNA profiling of beta cells of at least 1 CPM (counts per million) (31). Protein categories defined by Protein Atlas (20). Interacting proteins in the categories; nucleus, mitochondria, as well as those of undetermined category, are not visualized in this figure but are included in uploaded analysis. Increasing icon size depicts increasing significance. Gray lines depict previously reported protein:protein interactions and line thickness reflects confidence score (22).

Figure 2

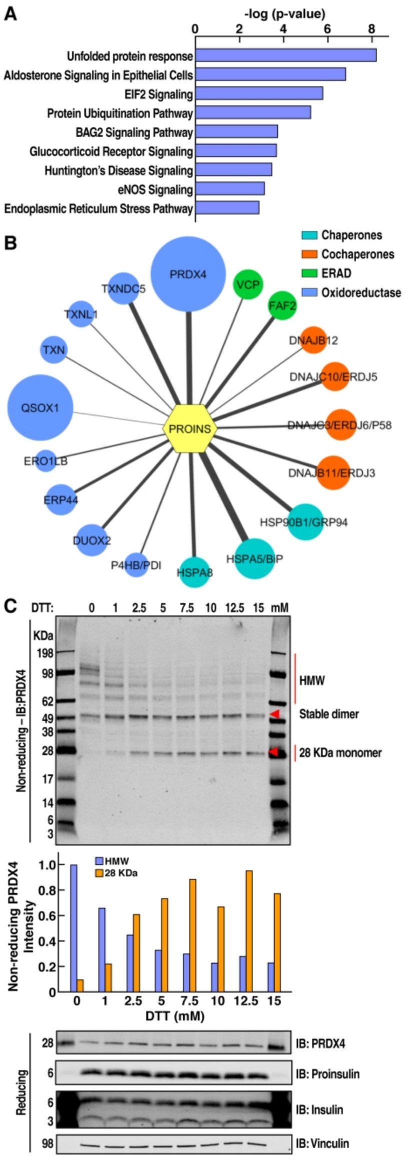

Figure 2- Human proinsulin interacts with ER resident folding factors, including PRDX4. (A) Ingenuity Pathway Analysis (IPA) of identified proinsulin interactors (not included are mitochondrial and ribosomal proteins) reveals enrichment of Unfolded Protein Response as a major pathway involved in proinsulin biosynthesis. (B) Proinsulin interacting ER resident folding factors with p value ≤0.05. Icon size reflects log2FC proinsulin IP/IgG IP and line thickness represents increasing significance (decreasing p values). (C) PRDX4 conformational analysis in normal murine islets. Live islets treated with a gradient of DTT concentrations ranging from 1 to 15 mM for 20 minutes (or untreated control (0), left lane) were lysed and resolved by non-reducing SDS-PAGE immunoblotted for PRDX4 and by reducing SDS-PAGE immunoblotted for PRDX4, proinsulin, insulin and vinculin. Intensity of disulfide linked HMW complex (size indicated 49 – 198 kDa) versus PRDX4 monomer (28 kDa) is quantified in graph. Molecular weight markers are shown.

Figure 3

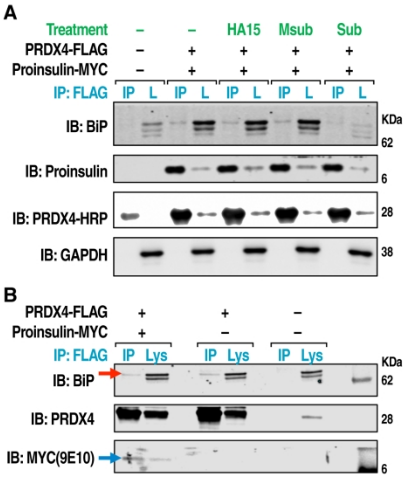

Figure 3- PRDX4 interacts with proinsulin and BiP, independent of each other. (A) HEK293T cells were transfected with plasmids expressing human Proinsulin-MYC and human PRDX4-FLAG or untransfected. After 44 hours cells were treated with SubAb that cleaves BiP (Sub, 2 µg/mL, 4 hrs), Mutant SubAb as control (Msub, 2 µg/mL, 4 hrs), the BiP inhibitor HA15 (10 µM, 4 hrs) or untreated, followed by cell lysis and immunoprecipitation with anti-FLAG magnetic beads. 3% of Lysate (L) and 20% of immunoprecipitate (IP) were analyzed on reducing SDS-PAGE. Note, antibody light chain band appears just below PRDX4. (B) HEK293A cells were transfected with equal amounts of total plasmid in combination of control pCDNA (-), human Proinsulin-MYC and human PRDX4-FLAG. Resulting lysates were subject to immunoprecipitation with anti-FLAG magnetic beads. Lysates (L) and IP fractions were immunoblotted for BiP, PRDX4 or MYC tag (proinsulin). Red arrows identifies BiP and blue arrow identifies Proinsulin-MYC band.

Figure 4

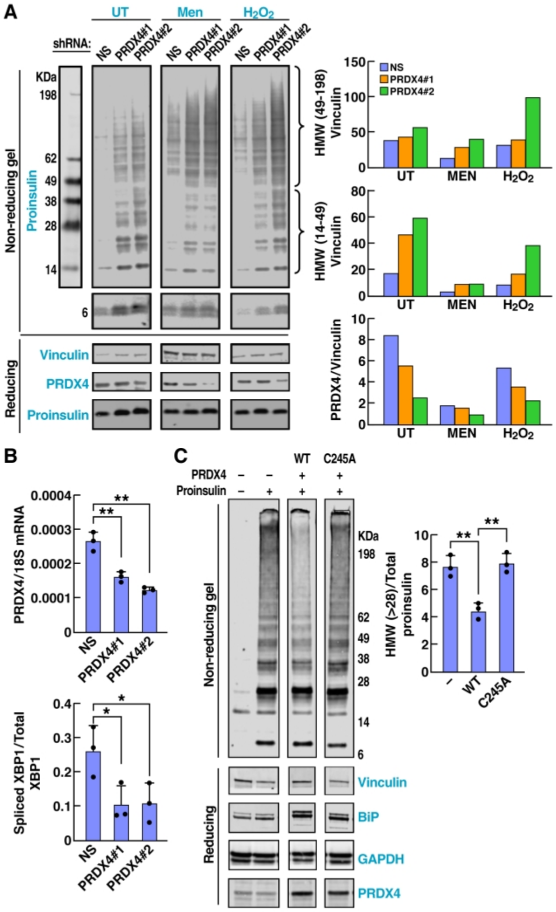

Figure 4- PRDX4 facilitates proinsulin folding. (A) Loss of PRDX4 increases proinsulin misfolding. PRDX4 was knocked down in MIN6 cells by stable expression of PRDX4 shRNA (PRDX4#1 and PRDX4#2),or scrambled non-specific shRNA (NS). Cells were untreated or treated with the oxidant menadione (Men) (100 μM, 1 hr) or H2O2 (1 mM, 1 hr). Non-reducing SDS-PAGE were immunoblotted with proinsulin antibody CCI17. Bottom panels of non-reducing gel shows darker exposure of proinsulin monomer band at approximately 6KDa. Reducing gels were immunoblotted for Vinculin, PRDX4, and total Proinsulin. Accompanying graphs (right) show quantification of HMW proinsulin bands from 14 – 49 KDa or 49 – 198 KDa from non-reducing gel and total PRDX4 from reducing gel, normalized by Vinculin. The data are representative of 4 independent experiments.(B) mRNA derived from cells described in (A) confirms PRDX4 knockdown in MIN6 stably expressed PRDX4 shRNA by qPCR using 3 biological replicates per line. Lower panel: qPCR analysis of the ER stress marker 'spliced XBP1' relative to total XBP1 was under-represented in the PRDX4 knockdown. (C) HEK293T cells were transfected with equal amounts of plasmids containing combinations of human Proinsulin-MYC, human WT-PRDX4, human PRDX4 harboring a mutation in the resolving cysteine (C245A-PRDX4) and GFP, or untransfected. Resulting lysates were analyzed by non- reducing and reducing SDS-

PAGE. Accompanying graph showed ratios of disulfide-bonded high molecular weight complexes (MW >28) over corresponding total proinsulin intensity determined on reducing gel. **p<0.01.

Figure 5

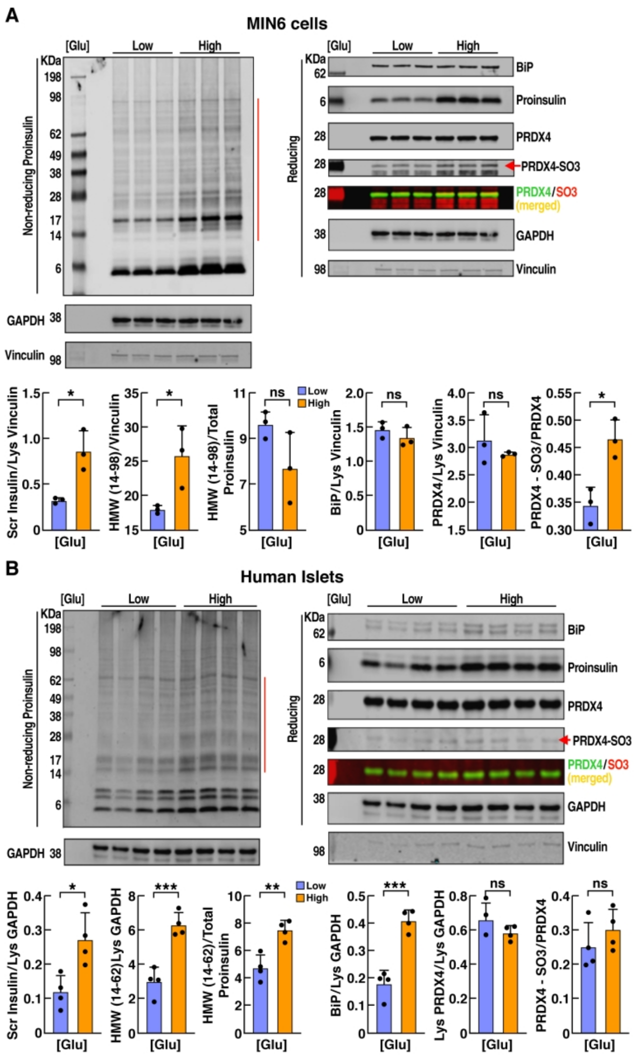

Figure 5- Analysis of high glucose induced proinsulin misfolding and PRDX4 expression in MIN6 and human islets. (A) MIN6 cells were glucose starved for 1 hour and then treated with Low (2.2 mM, n=3) or High (22 mM, n=3) glucose [Glu] for 22.5 hours. HMW proinsulin complexes (red bar) were resolved on non-reducing SDS-PAGE. Samples were also analyzed on reducing SDS-PAGE and immunoblotted for BiP, total proinsulin, PRDX4, and PRDX-SO3 along with loading controls (Vinculin and GAPDH). PRDX4 and PRDX-SO3 were immunoblotted with two different primary and secondary antibodies on the same membrane and the images were merged. Red arrow shows PRDX4-SO3 band identified by the PRDX-SO3 antibody. Accompanying graphs show secreted (scr) insulin assayed by ELISA in the media relative to Vinculin in lysate (Lys), HMW proinsulin complexes in lysate (red bar) to Vinculin, HMW proinsulin complexes (red bar) in lysate to total proinsulin, BiP to Vinculin, total PRDX4 to Vinculin, and PRDX4-SO3 band normalized to total PRDX4. (B) Human islets were glucose starved for 1 hour prior to treatment with Low (3 mM, n=4) or High (30 mM, n=4) glucose [Glu] for 18 hours. HMW proinsulin complexes (red bar) were resolved on non-reducing SDS-PAGE. Samples were analyzed on reducing and non-reducing SDS-PAGE as described in (A). Accompanying graphs are as described in A except that GAPDH is used to normalize secreted insulin, HMW proinsulin, and

PRDX4 instead of vinculin.

Figure 6

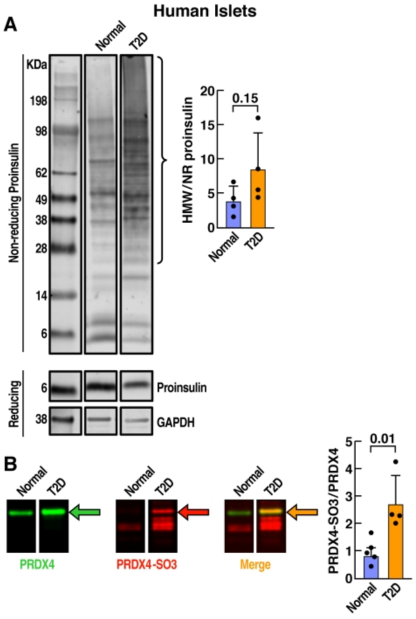

Figure 6- T2D islets exhibit increased PRDX4 sulfonylation. (A) 8.55 µg of protein from human islet preparations from 4 normal individuals and 4 patients with Type 2 Diabetes (T2D) were analyzed by non-reducing SDS-PAGE (upper panel) and immunoblotted for proinsulin (one representative sample is displayed here). The accompanying graph shows quantification of HMW bands (size range indicated by curved bracket) normalized by proinsulin monomer on the non-reducing gel for all 8 samples. Reducing gels were immunoblotted for total proinsulin and GAPDH loading control (bottom panels). (B) All samples were immunoblotted for both PRDX4 (green) and sulfonylated PRDXs (i.e. PRDX-SO3, red) on the same membrane. Merged image shows co-localization of PRDX4 band with its sulfonylated version at the same molecular weight. Intensity of the sulfonylated PRDX4 bands (yellow arrow) versus total PRDX4 were quantified.

Unbiased profiling of the human proinsulin biosynthetic interaction network reveals a role for peroxiredoxin 4 in proinsulin folding

Short running title: Human proinsulin biosynthetic interaction network

Authors: Duc T. Tran*[1], Anita Pottekat*[3,10], Saiful A. Mir[1,9], Salvatore Loguercio[4], Insook Jang[3], Alexandre Rosa Campos[8], Kathleen M. Scully[1], Reyhaneh Lahmy[1,11], Ming Liu[6,7], Peter Arvan[6], William E. Balch[4,5], Randal J. Kaufman[3§], Pamela Itkin-Ansari[1,2§]

*** These authors contributed equally to this work**

[1] Development, Aging and Regeneration program, Sanford Burnham Prebys Medical Discovery Institute, La Jolla, USA
[2] Department of Pediatrics, University of California, San Diego, La Jolla, CA, USA
[3] Degenerative Diseases Program, Sanford Burnham Prebys Medical Discovery Institute, La Jolla, USA
[4] The Scripps Research Institute, Department of Molecular Medicine, La Jolla, CA, USA
[5] Integrative Structural and Computational Biology, The Scripps Research Institute, La Jolla, CA, USA
[6] Division of Metabolism, Endocrinology & Diabetes, University of Michigan Medical School, Ann Arbor, USA
[7] Department of Endocrinology and Metabolism, Tianjin Medical University, Tianjin, China
[8] Sanford Burnham Prebys Medical Discovery Institute Proteomic Core, La Jolla, CA, USA
[9] Current address School of Medicine, University of California at San Diego, La Jolla, USA
[10] Current address Illumina, San Diego, CA, USA
[11] Current address OncoMed Pharmaceuticals, Inc, Redwood City, CA, USA

§Corresponding authors

Pamela Itkin-Ansari, PhD

Adjunct Associate Professor
Sanford Burnham Prebys Medical Discovery Institute
Joint appointment-UCSD
Tel: 858-646-3100 x 3428
Email: pitkin@sbpdiscovery.org

Randal J Kaufman

Director and Professor Degenerative Diseases Program
Endowed Chair of Cell Biology
Sanford Burnham Prebys Medical Discovery Institute
Tel: 858.795.5149
Email: rkaufman@sbpdiscovery.org

Supplemental Figure Legends

Figure S1 - Specificity of monoclonal antibody 20G11 to proinsulin. (A) Lysates from human islets immunoprecipitated with in-house generated monoclonal antibody 20G11 to proinsulin or insulin antibody. Note negligible precipitation of insulin by 20G11. B) WT proinsulin, proinsulin MIDY mutants (A, B, C) or GFP (G) were overexpressed in COS1 cells and immunoprecipitated and immunoblotted with 20G11 antibody. The upper band in the lysate may be preproinsulin, recognized by 20G11 in reduced form (but not in native form in IP).

Figure S2 - Comparison of Label Free and TMT Mass Spectrometric analysis on one islet preparation identified common proteins but with different sensitivities.

Figure S3- MS/MS Proinsulin Interactions Validated by IP-western blot. (A) Validation of MYO18A interaction with proinsulin was performed by proinsulin immunoprecipitation of lysates from human islets. 4% of lysate and supernatant, and 12% IP were analyzed by reducing SDS-PAGE and immunoblotted for MYO18A. (B) Validation of BiP, ERDJ5, GRP94 interaction with proinsulin was performed by immunoprecipitation of proinsulin from human islet lysate with proinsulin specific primary antibody (20G11) or mouse IgG. Lysates and Supernatants (Sup) 5%, and IP 12% were resolved on SDS-PAGE. Membranes were cut according to molecular weight markers and blotted for the indicated primary antibodies: BIP, ERDJ5, GRP94. (C) HEK293A cells were transfected with plasmids expressing WT human Proinsulin-MYC, human Akita mutant Proinsulin-MYC, human PRDX4-FLAG or pCDNA. Lysates were immunoprecipitated with anti-MYC (tag)-beads or anti-FLAG (tag)-beads. Lysates and supernatants 5%, and IPs 15% were immunoblotted for PRDX4, FLAG, human proinsulin (20G11) and MYC (tag).

Figure S4- PRDX4 mRNA expression in human beta cell single cell RNA-seq analysis is shown compared to insulin and the beta cell transcription factor PDX1 (22). Note that insulin is on a log scale.

Figure S5- PRDX4 immunoprecipitation controls for Figure 3A. (A) Briefly HEK293T cells were transfected with combinations of Proinsulin-MYC, PRDX4-FLAG and GFP. After 44 hours cells were treated with SubAb (2 µg/mL, 4 hrs), Mutant SubAb (2 µg/mL, 4 hrs), HA15 (10 µM, 4 hrs) or untreated, followed by immunoprecipitation with anti-FLAG magnetic beads. Non-reducing SDS-PAGE of PRDX4 immunoprecipitated with anti-FLAG beads immunoblotted with PRDX4-HRP direct conjugate antibody. The data shows that all PRDX4 conformations were immunoprecipitated (20% of IP analyzed). (B) The same experimental conditions described above except that control GFP was transfected in place of PRDX4-FLAG. Lysates were immunoprecipitated with anti-FLAG beads, showing that no proinsulin or BiP binds non-specifically to FLAG beads.

Figure S6- Menadione induces proinsulin misfolding and recruits PRDX4 into HMW complexes in human islets. One thousand human islet equivalents were treated with either 100 or 200 µM Menadione for 1 hour at 37^{o}C and lysed with 2X Laemmli without BME and analyzed on reducing and non-reducing SDS-PAGE. Left panel shows non-reducing SDS-PAGE immunoblotted for proinsulin and its accompanying reducing SDS-PAGE immunoblotted for loading control vinculin, PRDX4 and proinsulin. Right panel shows non-reducing SDS-PAGE immunoblotted for PRDX4 and its accompanying reducing SDS-PAGE for vinculin, PRDX4, and proinsulin.

Figure S1. Specificity of monoclonal antibody 20G11 to proinsulin.

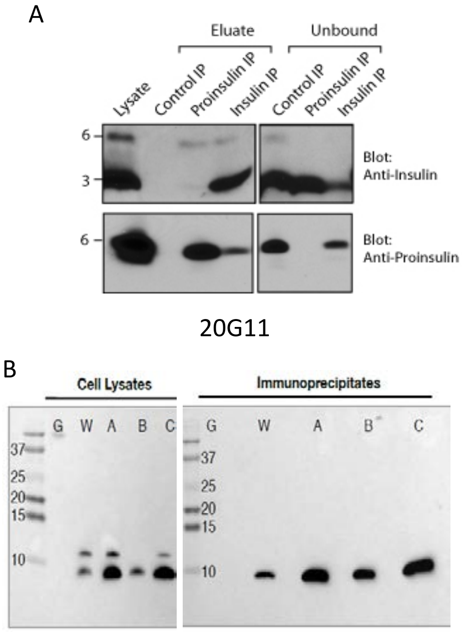

G – GFP; **W** – WT; **A** – Akita [C(A7)Y]; **B** – LY(B15,16)H; **C** – C(A6)Y

Figure S2. Comparison of Label Free and TMT analysis in human islets.

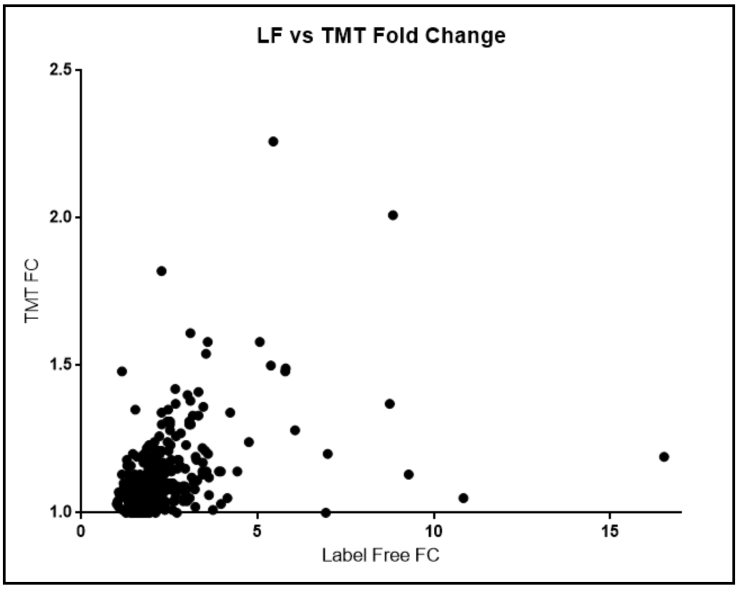

Figure S3. MS/MS Proinsulin Interactions Validated by IP-western blot.

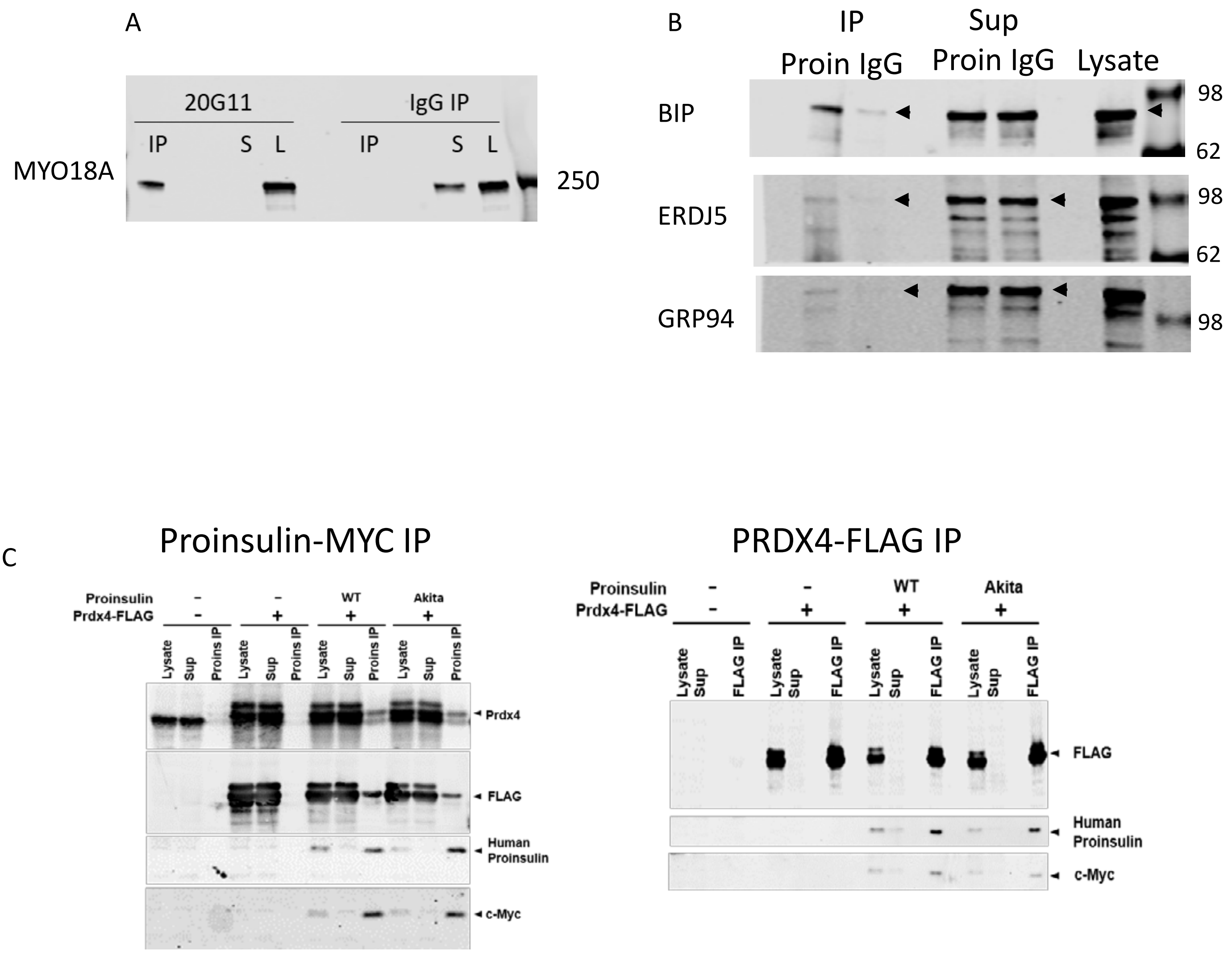

Figure S4. PRDX4 mRNA expression in human beta cell single cell RNA-seq analysis.

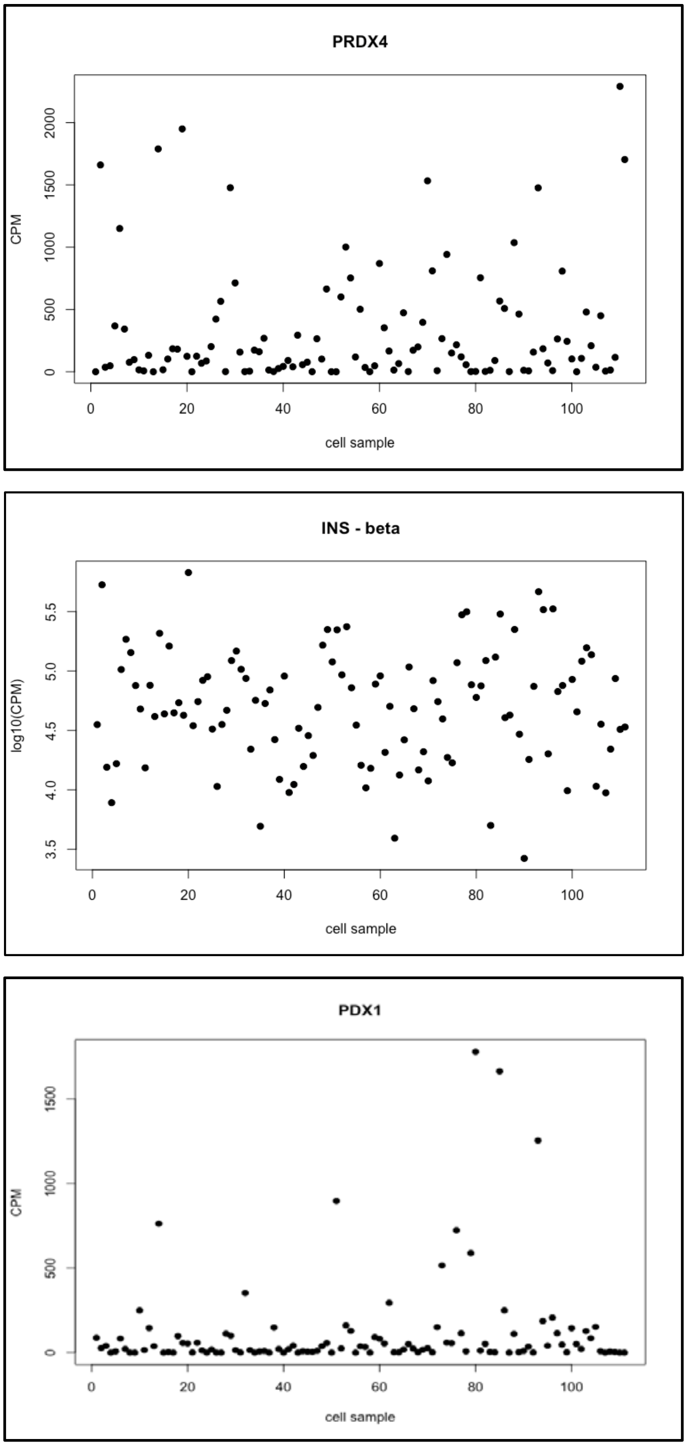

Figure S5. PRDX4 immunoprecipitation controls for Figure 3A.

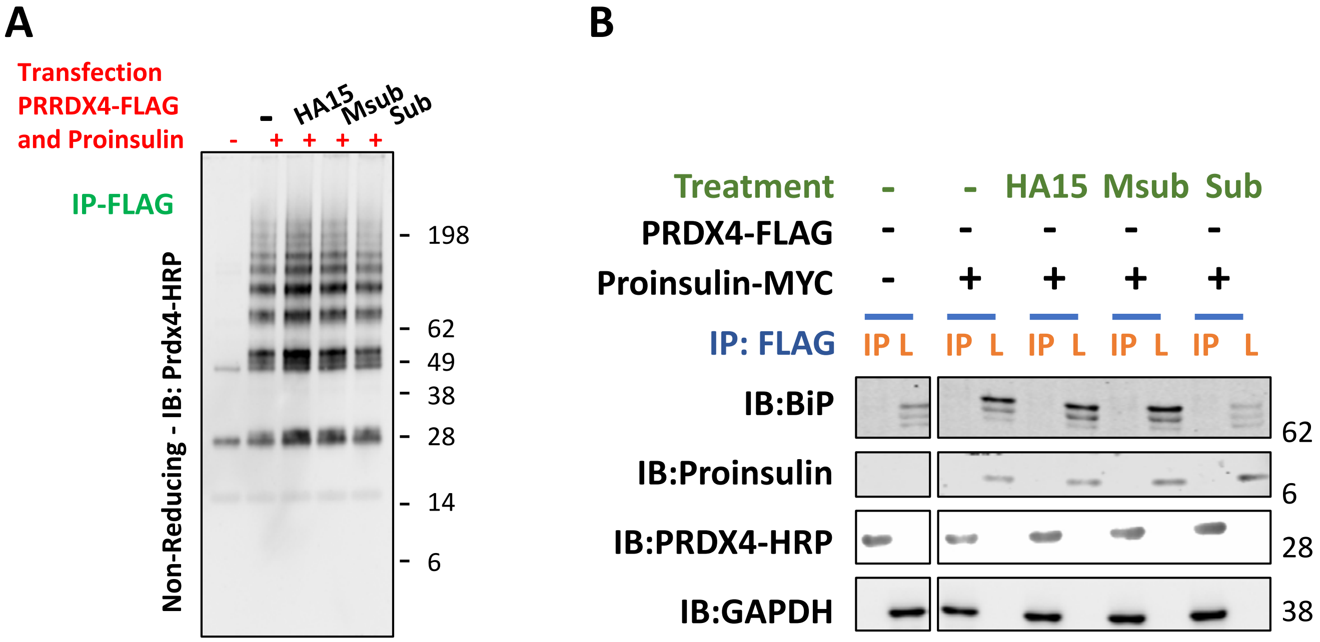

Figure S6. Menadione induces proinsulin misfolding and recruits PRDX4 into HMW complexes in human islets.

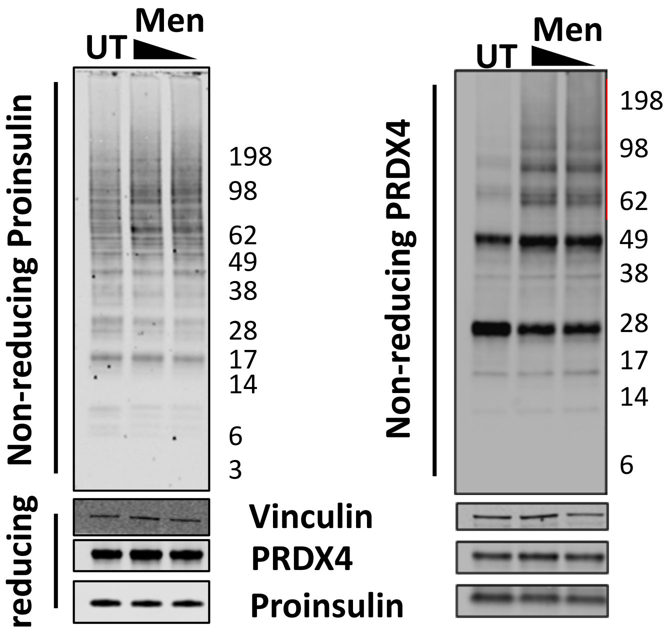

Supplementary table 1 - Primary antibodies

	Antibodies	**Source**	**Product Number**	**Species**
1	Anti-Grp94	Cell Signaling Technology	20292P	Rabbit monoclonal
2	Anti-mouse BiP	Dr Linda Hendershot's Lab		Rabbit monoclonal
3	Anti-human BiP	Cell Signaling Technology	(C50B12) 3177	Rabbit
4	Anti-ERDJ5	ProteinTech	13101-1-AP	Rabbit Polyclonal
5	Anti-PRDX4	R&D System	AF5460	Goat Polyclonal
6	Anti-PRDX4-HRP	LSBio	LS-C713462	Rabbit Polyclonal
7	Anti-PRDX-SO3	Abcam	ab16830	Rabbit polyclonal
8	Anti-rat proinsulin (CCI-17)	Hystest	2PR8	Mouse monoclonal
9	Anti-Myo18	ProteinTech	14611	Rabbit polyclonal
10	Anti-GAPDH-HRP	GeneTex	GTX627408-01	Mouse
11	Anti-Myc tag	Abcam	ab32	Mouse
12	Anti-rabbit vinculin	ProteinTech	66305-1-lg	Mouse monoclonal
13	Anti-vinculin	Cell Signaling Technology	4650S	Rabbit
14	Anti-human proinsulin (20G11)	Dr William E. Balch's Lab		Mouse monoclonal
15	Anti-insulin	Dr Peter Arvan's Lab		Guinea pig

Dilution Factor
1/1000
1/1000
1/1000
1/1000
1/1000
1/1000
1/1000
1/10,000
1/1000
1/100,000
1/1000
1/1000
1/1000
1/1000
1/1000

Supplementary Table 2 - Proinsulin Interactome in normal human islets

	Description
IU	Normal Human Islets immunoprecipitated by proinsulin specific antibody 20G11-conjuga
CU	Normal Human Islets control immunoprecipitation by mouse IgG-conjugated beads
beta	Confirmed expression in single cell RNA-seq data (Ref 22)

ted beads

EID	Protein	Genenames	Proteinnames	foundExp_	log2FC_IU_vs_CU
10005	O14734	ACOT8	Acyl-coenzyme A thioesterase 8	2	2.096825632
10061	Q9UG63	ABCF2	ATP-binding cassette sub-family F m	5	1.611339984
10075	Q7Z6Z7	HUWE1	E3 ubiquitin-protein ligase HUWE1	32	1.046519163
10085	O43854	EDIL3	EGF-like repeat and discoidin I-like d	1	1.661199817
10113	Q9HCU5	PREB	Prolactin regulatory element-bindin	4	1.050438352
10136	P09093	CELA3A	Chymotrypsin-like elastase family m	1	1.26926769
1020	Q00535	CDK5	Cyclin-dependent-like kinase 5	15	1.770296026
10294	O60884	DNAJA2	DnaJ homolog subfamily A member	57	1.169612852
10380	O95861	BPNT1	3(2),5-bisphosphate nucleotidase 1	5	1.288546153
10399	P63244	GNB2L1	Guanine nucleotide-binding protein	75	1.306095157
10432	Q96PK6	RBM14	RNA-binding protein 14	77	1.518967531
10463	Q6PML9	SLC30A9	Zinc transporter 9	0	1.387515073
10528	O00567	NOP56	Nucleolar protein 56	53	1.114436169
10549	Q13162	PRDX4	Peroxiredoxin-4	101	6.171853493
10555	O15120	AGPAT2	1-acyl-sn-glycerol-3-phosphate acylt	0	1.491853132
10562	Q6UX06	OLFM4	Olfactomedin-4	0	1.01076287
10611	Q96HC4	PDLIM5	PDZ and LIM domain protein 5	8	1.224278254
10612	O75382	TRIM3	Tripartite motif-containing protein 3	0	1.261714778
10629	Q9Y6J9	TAF6L	TAF6-like RNA polymerase II p300/C	2	1.313720541
10670	Q7L523	RRAGA	Ras-related GTP-binding protein A	1	1.074745159
10726	Q9Y266	NUDC	Nuclear migration protein nudC	47	1.15247803
1075	P53634	CTSC	Dipeptidyl peptidase 1;Dipeptidyl pe	1	1.709169319
10767	Q9Y450	HBS1L	HBS1-like protein	8	1.022483797
10788	Q13576	IQGAP2	Ras GTPase-activating-like protein IQ	13	1.778899264
10908	Q8IY17	PNPLA6	Neuropathy target esterase	6	1.387051165
10916	Q9UNF1	MAGED2	Melanoma-associated antigen D2	21	1.499358192
10949	Q13151	HNRNPA0	Heterogeneous nuclear ribonucleop	100	1.518953911
10952	P60468	SEC61B	Protein transport protein Sec61 sub	3	1.645113527
10971	P27348	YWHAQ	14-3-3 protein theta	92	1.176399142
10982	Q15555	MAPRE2	Microtubule-associated protein RP/	0	1.230732904
10999	Q6P1M0	SLC27A4	Long-chain fatty acid transport prot	2	1.428608479
11047	Q16186	ADRM1	Proteasomal ubiquitin receptor ADR	18	1.383135817
11076	O94811	TPPP	Tubulin polymerization-promoting p	1	1.824214166
11100	Q9BUJ2	HNRNPUL1	Heterogeneous nuclear ribonucleop	66	1.092769497
11187	Q9Y446	PKP3	Plakophilin-3	4	1.530023087
11188	Q9Y2I1	NISCH	Nischarin	3	1.231730772
11217	Q9Y2D5	AKAP2	A-kinase anchor protein 2	10	2.036486071
11261	Q99653	CHP1	Calcineurin B homologous protein 1	0	2.262484073
112724	Q8NBN7	RDH13	Retinol dehydrogenase 13	1	1.158239775
112858	Q96S44	TP53RK	TP53-regulating kinase	4	1.339391673
11315	Q99497	PARK7	Protein deglycase DJ-1	29	1.007825197
113251	Q71RC2	LARP4	La-related protein 4	13	1.29964941
113612	Q7Z449	CYP2U1	Cytochrome P450 2U1	0	1.583960307
1153	Q14011	CIRBP	Cold-inducible RNA-binding protein	73	2.366207598
115817	Q96LJ7	DHRS1	Dehydrogenase/reductase SDR fami	0	1.720348078
116113	Q8IVH2	FOXP4	Forkhead box protein P4	3	1.179078921
1186	P51798	CLCN7	H(+)/Cl(-) exchange transporter 7	0	1.364820476
118881	Q86VU5	COMTD1	Catechol O-methyltransferase doma	2	1.127725064
1191	P10909	CLU	Clusterin;Clusterin beta chain;Cluste	6	1.022338453
123263	Q96DP5	MTFMT	Methionyl-tRNA formyltransferase,	0	2.604040506
125950	Q8IY67	RAVER1	Ribonucleoprotein PTB-binding 1	13	1.288456472
1267	P09543	CNP	2,3-cyclic-nucleotide 3-phosphodies	16	1.461116806
127262	Q5T0D9	TPRG1L	Tumor protein p63-regulated gene 1	0	1.915604098

127829	Q96BM9	ARL8A	ADP-ribosylation factor-like protein	1	1.308915563
131118	Q96DA6	DNAJC19	Mitochondrial import inner membra	1	1.051196095
132001	Q96BW9	TAMM41	Phosphatidate cytidylyltransferase,	0	2.079875155
1337	P12074	COX6A1	Cytochrome c oxidase subunit 6A1,	2	2.356631667
1374	P50416	CPT1A	Carnitine O-palmitoyltransferase 1,	1	1.007320199
137492	Q8NEZ2	VPS37A	Vacuolar protein sorting-associated	0	2.444091827
139322	Q6UXV4	APOOL	MICOS complex subunit MIC27	2	1.382315866
1400	Q14194	CRMP1	Dihydropyrimidinase-related protei	20	1.55699028
140823	P60602	ROMO1	Reactive oxygen species modulator	0	1.47150433
143098	Q5T2T1	MPP7	MAGUK p55 subfamily member 7	4	1.831482985
1452	P48729	CSNK1A1	Casein kinase I isoform alpha	12	1.097197205
1476	P04080	CSTB	Cystatin-B	36	1.286622414
1508	P07858	CTSB	Cathepsin B;Cathepsin B light chain;	5	1.397823346
152100	Q7Z7K0	CMC1	COX assembly mitochondrial protei	0	1.388275159
1537	P08574	CYC1	Cytochrome c1, heme protein, mito	8	1.097776166
1593	Q02318	CYP27A1	Sterol 26-hydroxylase, mitochondri	0	1.63173588
1655	P17844	DDX5	Probable ATP-dependent RNA helica	182	1.170886898
166785	Q8IVH4	MMAA	Methylmalonic aciduria type A prot	0	1.705255004
1915	P68104	EEF1A1	Elongation factor 1-alpha 1	0	1.139156223
1962	Q08426	EHHADH	Peroxisomal bifunctional enzyme;E	0	1.230223737
1975	P23588	EIF4B	Eukaryotic translation initiation fact	111	3.975178296
1983	P55010	EIF5	Eukaryotic translation initiation fact	9	2.529768977
1994	Q15717	ELAVL1	ELAV-like protein 1	65	1.431085154
200186	Q53ET0	CRTC2	CREB-regulated transcription coacti	0	1.599992676
2109	P38117	ETFB	Electron transfer flavoprotein subu	10	1.877401907
2130	Q01844	EWSR1	RNA-binding protein EWS	99	1.257182611
2193	Q9Y285	FARSA	Phenylalanine--tRNA ligase alpha su	30	1.419442808
22	O75027	ABCB7	ATP-binding cassette sub-family B m	3	1.11350704
220988	P51991	HNRNPA3	Heterogeneous nuclear ribonucleop	124	1.296435868
221092	Q1KMD3	HNRNPUL2	Heterogeneous nuclear ribonucleop	33	1.114537613
2232	P22570	FDXR	NADPH:adrenodoxin oxidoreductas	5	1.236252161
22803	Q9H0D6	XRN2	5-3 exoribonuclease 2	50	1.423518999
22827	Q9UHX1	PUF60	Poly(U)-binding-splicing factor PUF6	93	4.933175164
22848	Q2M2I8	AAK1	AP2-associated protein kinase 1	3	1.199323889
22884	Q9Y2I8	WDR37	WD repeat-containing protein 37	0	1.362730634
22907	Q7L2E3	DHX30	Putative ATP-dependent RNA helica	42	1.265151071
23	Q8NE71	ABCF1	ATP-binding cassette sub-family F m	43	1.445007421
23011	Q9UL25	RAB21	Ras-related protein Rab-21	6	1.226231104
23071	Q9BS26	ERP44	Endoplasmic reticulum resident pro	10	1.585073039
23151	Q6IC98	GRAMD4	GRAM domain-containing protein 4	0	1.078555598
2316	P21333	FLNA	Filamin-A	158	1.094985427
2317	O75369	FLNB	Filamin-B	108	1.018895921
23172	Q15018	FAM175B	BRISC complex subunit Abro1	0	1.060117289
23185	Q92615	LARP4B	La-related protein 4B	5	1.288586385
23193	Q14697	GANAB	Neutral alpha-glucosidase AB	63	1.035637982
23196	Q9NZB2	FAM120A	Constitutive coactivator of PPAR-ga	15	1.284491314
23197	Q96CS3	FAF2	FAS-associated factor 2	6	1.377045929
23242	O75128	COBL	Protein cordon-bleu	1	1.118124912
23303	Q9NQT8	KIF13B	Kinesin-like protein KIF13B	0	1.2955024
23312	Q8TDJ6	DMXL2	DmX-like protein 2	0	1.205767949
23335	Q9Y4E6	WDR7	WD repeat-containing protein 7	2	1.051006948
23367	Q6PKG0	LARP1	La-related protein 1	0	1.002993229
23387	Q9Y2K2	SIK3	Serine/threonine-protein kinase SIK	1	1.23306372
23408	Q9NXA8	SIRT5	NAD-dependent protein deacylase s	0	1.851904598

23424	Q8NHU6	TDRD7	Tudor domain-containing protein 7	0	1.212416632
23435	Q13148	TARDBP	TAR DNA-binding protein 43	42	1.086411246
23463	O60725	ICMT	Protein-S-isoprenylcysteine O-methy	1	1.460973163
23589	Q9Y2V2	CARHSP1	Calcium-regulated heat stable prote	1	1.174975519
23597	Q9Y305	ACOT9	Acyl-coenzyme A thioesterase 9, mit	2	1.10958736
23753	Q9HCN8	SDF2L1	Stromal cell-derived factor 2-like pro	4	1.068771423
23761	Q9UG56	PISD	Phosphatidylserine decarboxylase p	0	1.33908282
23787	Q9NZJ7	MTCH1	Mitochondrial carrier homolog 1	13	1.029169868
24139	O95834	EML2	Echinoderm microtubule-associated	2	1.02660648
2539	P11413	G6PD	Glucose-6-phosphate 1-dehydrogen	14	1.124905585
255743	Q6UXI9	NPNT	Nephronectin	0	2.106293945
25797	Q16769	QPCT	Glutaminyl-peptide cyclotransferase	51	1.38895465
25873	Q9Y3U8	RPL36	60S ribosomal protein L36	78	1.483807855
25874	O95563	MPC2	Mitochondrial pyruvate carrier 2	1	1.229146199
25939	Q9Y3Z3	SAMHD1	Deoxynucleoside triphosphate triph	13	1.110021351
25979	Q6IAN0	DHRS7B	Dehydrogenase/reductase SDR fami	4	1.292642613
26090	Q8N2K0	ABHD12	Monoacylglycerol lipase ABHD12	1	1.092042098
26092	Q5JTV8	TOR1AIP1	Torsin-1A-interacting protein 1	4	1.41520568
26119	Q5SW96	LDLRAP1	Low density lipoprotein receptor ad	0	2.494300546
26135	Q8NC51	SERBP1	Plasminogen activator inhibitor 1 RN	108	1.101188085
2620	O43903	GAS2	Growth arrest-specific protein 2	5	1.250058575
26275	Q6NVY1	HIBCH	3-hydroxyisobutyryl-CoA hydrolase,	2	1.125094022
26286	Q9NP61	ARFGAP3	ADP-ribosylation factor GTPase-acti	1	1.701693545
2641	P01275	GCG	Glucagon;Glicentin;Glicentin-related	0	1.136542627
2673	Q06210	GFPT1	Glutamine--fructose-6-phosphate ar	9	1.076214711
2677	P38435	GGCX	Vitamin K-dependent gamma-carbo	1	8.74202052
27089	O14949	UQCRQ	Cytochrome b-c1 complex subunit 8	3	1.631377031
27161	Q9UKV8	AGO2	Protein argonaute-2	22	1.337529097
27183	Q9UN37	VPS4A	Vacuolar protein sorting-associated	5	1.253365508
27238	Q92917	GPKOW	G patch domain and KOW motifs-co	10	1.315316482
2745	P35754	GLRX	Glutaredoxin-1	1	1.219718514
2794	P36915	GNL1	Guanine nucleotide-binding protein-	2	1.585429736
285282	Q5HYI8	RABL3	Rab-like protein 3	3	1.10767733
2887	Q13322	GRB10	Growth factor receptor-bound prote	1	2.723298575
29085	Q9NRX4	PHPT1	14 kDa phosphohistidine phosphata	0	1.615687612
29087	Q9P016	THYN1	Thymocyte nuclear protein 1	0	1.157001966
291	P12235	SLC25A4	ADP/ATP translocase 1	136	1.656625179
2969	P78347	GTF2I	General transcription factor II-I	75	1.208376922
29926	Q96IJ6	GMPPA	Mannose-1-phosphate guanyltransf	3	1.858705425
29957	Q6NUK1	SLC25A24	Calcium-binding mitochondrial carri	4	1.183320201
29974	Q9NQ94	A1CF	APOBEC1 complementation factor	0	1.435503707
3032	P55084	HADHB	Trifunctional enzyme subunit beta,	23	1.033841448
3035	P12081	HARS	Histidine--tRNA ligase, cytoplasmic	18	2.030739396
3094	P49773	HINT1	Histidine triad nucleotide-binding pr	13	2.154902373
3146	P09429	HMGB1	High mobility group protein B1	65	1.674569275
3155	P35914	HMGCL	Hydroxymethylglutaryl-CoA lyase, m	1	1.690419096
3170	Q9Y261	FOXA2	Hepatocyte nuclear factor 3-beta	0	1.518657707
318	P50583	NUDT2	Bis(5-nucleosyl)-tetraphosphatase [	0	1.32509208
3183	P07910	HNRNPC	Heterogeneous nuclear ribonucleop	127	1.564352285
3184	Q14103	HNRNPD	Heterogeneous nuclear ribonucleop	153	1.176746387
3191	P14866	HNRNPL	Heterogeneous nuclear ribonucleop	133	1.076976512
3192	Q00839	HNRNPU	Heterogeneous nuclear ribonucleop	212	1.155259211
3309	P11021	HSPA5	78 kDa glucose-regulated protein	292	2.593403089
3312	P11142	HSPA8	Heat shock cognate 71 kDa protein	328	1.570637474

3313	P38646	HSPA9	Stress-70 protein, mitochondrial	239	1.457035805
3418	P48735	IDH2	Isocitrate dehydrogenase [NADP], m	11	1.145742446
3420	O43837	IDH3B	Isocitrate dehydrogenase [NAD] sub	7	1.035768125
349565	Q96T66	NMNAT3	Nicotinamide/nicotinic acid mononu	0	1.002155444
3630	P01308	INS	Insulin;Insulin B chain;Insulin A chai	0	7.033890797
3631	Q96PE3	INPP4A	Type I inositol 3,4-bisphosphate 4-p	1	1.300018003
374291	O75251	NDUFS7	NADH dehydrogenase [ubiquinone]	6	2.225187282
376497	Q6PCB7	SLC27A1	Long-chain fatty acid transport prot	0	1.156251455
3796	O00139	KIF2A	Kinesin-like protein KIF2A	18	1.098235064
3858	P13645	KRT10	Keratin, type I cytoskeletal 10	297	1.190340299
3875	P05783	KRT18	Keratin, type I cytoskeletal 18	182	1.47135655
3898	O00515	LAD1	Ladinin-1	0	1.391108523
391	P84095	RHOG	Rho-related GTP-binding protein Rh	7	1.378730022
3921	P08865	RPSA	40S ribosomal protein SA	103	1.000029713
3959	Q08380	LGALS3BP	Galectin-3-binding protein	16	1.109112935
3980	P49916	LIG3	DNA ligase 3	12	1.536530111
3993	Q6P1M3	LLGL2	Lethal(2) giant larvae protein homol	0	1.013012492
399687	Q92614	MYO18A	Unconventional myosin-XVIIIa	11	3.710111906
400	P40616	ARL1	ADP-ribosylation factor-like protein	14	1.374778387
4008	Q8WWI1	LMO7	LIM domain only protein 7	17	1.625500148
4082	P29966	MARCKS	Myristoylated alanine-rich C-kinase	47	2.146517753
4128	P21397	MAOA	Amine oxidase [flavin-containing] A	0	1.432669379
4133	P11137	MAP2	Microtubule-associated protein 2	1	1.001279942
4144	P31153	MAT2A	S-adenosylmethionine synthase isof	34	1.089156352
421	O00192	ARVCF	Armadillo repeat protein deleted in	3	1.10495175
4247	Q10469	MGAT2	Alpha-1,6-mannosyl-glycoprotein 2-	0	1.345535857
4282	P14174	MIF	Macrophage migration inhibitory fa	27	1.170626251
4329	Q02252	ALDH6A1	Methylmalonate-semialdehyde deh	1	1.013545214
4430	O43795	MYO1B	Unconventional myosin-Ib	47	1.291754616
4615	Q99836	MYD88	Myeloid differentiation primary res	0	1.374799793
4637	P60660	MYL6	Myosin light polypeptide 6	126	1.839016876
4641	O00159	MYO1C	Unconventional myosin-Ic	60	1.146001022
4642	O94832	MYO1D	Unconventional myosin-Id	33	1.004230909
4646	Q9UM54	MYO6	Unconventional myosin-VI	29	1.15380358
4695	O43678	NDUFA2	NADH dehydrogenase [ubiquinone]	0	1.210279623
4697	O00483	NDUFA4	Cytochrome c oxidase subunit NDU	5	1.710810768
4698	Q16718	NDUFA5	NADH dehydrogenase [ubiquinone]	3	1.312988562
4700	P56556	NDUFA6	NADH dehydrogenase [ubiquinone]	3	1.165022234
4701	O95182	NDUFA7	NADH dehydrogenase [ubiquinone]	0	1.569175965
4702	P51970	NDUFA8	NADH dehydrogenase [ubiquinone]	0	1.326823621
4704	Q16795	NDUFA9	NADH dehydrogenase [ubiquinone]	15	1.17724611
4710	O95168	NDUFB4	NADH dehydrogenase [ubiquinone]	4	1.444192785
4719	P28331	NDUFS1	NADH-ubiquinone oxidoreductase 7	12	1.137391381
4723	P49821	NDUFV1	NADH dehydrogenase [ubiquinone]	3	1.710134115
4724	O43181	NDUFS4	NADH dehydrogenase [ubiquinone]	0	1.621334685
4725	O43920	NDUFS5	NADH dehydrogenase [ubiquinone]	1	1.310877546
4726	O75380	NDUFS6	NADH dehydrogenase [ubiquinone]	0	1.321755078
4729	P19404	NDUFV2	NADH dehydrogenase [ubiquinone]	2	1.006862277
4750	Q96PY6	NEK1	Serine/threonine-protein kinase Ne	0	1.364411077
476	P05023	ATP1A1	Sodium/potassium-transporting AT	67	1.38965853
4825	P78426	NKX6-1	Homeobox protein Nkx-6.1	0	1.201074267
4841	Q15233	NONO	Non-POU domain-containing octam	152	1.074720912
4904	P67809	YBX1	Nuclease-sensitive element-binding	184	1.305641743
50485	Q9NZC9	SMARCAL1	SWI/SNF-related matrix-associated	2	1.259542386

50488	Q8N4C8	MINK1	Misshapen-like kinase 1	4	1.280011503
50506	Q9NRD8	DUOX2	Dual oxidase 2	0	1.699000441
5052	Q06830	PRDX1	Peroxiredoxin-1	186	1.070340156
50814	Q15738	NSDHL	Sterol-4-alpha-carboxylate 3-dehydr	6	1.133218167
509	P36542	ATP5C1	ATP synthase subunit gamma, mitoc	33	1.346953769
51035	Q04323	UBXN1	UBX domain-containing protein 1	3	1.311561153
51065	Q71UM5	RPS27L	40S ribosomal protein S27-like	116	1.161785205
51070	Q9Y314	NOSIP	Nitric oxide synthase-interacting pro	3	1.322327233
51097	Q8NBX0	SCCPDH	Saccharopine dehydrogenase-like ox	2	1.693612422
51119	Q9Y3A5	SBDS	Ribosome maturation protein SBDS	9	1.08144509
51144	Q53GQ0	HSD17B12	Very-long-chain 3-oxoacyl-CoA redu	8	1.270168054
51164	Q9UJW0	DCTN4	Dynactin subunit 4	8	1.322143461
51204	Q9BSH4	TACO1	Translational activator of cytochrom	1	1.538545901
5122	P29120	PCSK1	Neuroendocrine convertase 1	1	1.474553173
51295	Q9BQ95	ECSIT	Evolutionarily conserved signaling in	0	1.011674313
51382	Q9Y5K8	ATP6V1D	V-type proton ATPase subunit D	0	1.499252466
51474	Q9UHB6	LIMA1	LIM domain and actin-binding prote	45	1.796836277
51510	Q9NZZ3	CHMP5	Charged multivesicular body protein	2	2.019548418
51534	Q9NP79	VTA1	Vacuolar protein sorting-associated	3	1.257299414
5160	P08559	PDHA1	Pyruvate dehydrogenase E1 compor	25	1.37904592
5165	Q15120	PDK3	[Pyruvate dehydrogenase (acetyl-tra	2	1.147136246
51651	Q9Y3E5	PTRH2	Peptidyl-tRNA hydrolase 2, mitocho	7	1.762163078
51678	Q9NZW5	MPP6	MAGUK p55 subfamily member 6	3	1.056343959
51699	Q9UBQ0	VPS29	Vacuolar protein sorting-associated	7	1.02239817
51726	Q9UBS4	DNAJB11	DnaJ homolog subfamily B member	27	1.909784571
51741	Q9NZC7	WWOX	WW domain-containing oxidoreduct	0	1.759526349
5188	O75879	GATB	Glutamyl-tRNA(Gln) amidotransfera	0	1.279384
5213	P08237	PFKM	ATP-dependent 6-phosphofructokin	17	1.074435487
5250	Q00325	SLC25A3	Phosphate carrier protein, mitochor	79	1.20233069
5300	Q13526	PIN1	Peptidyl-prolyl cis-trans isomerase N	11	2.517175687
5315	P14618	PKM	Pyruvate kinase PKM	181	1.036220633
539	P48047	ATP5O	ATP synthase subunit O, mitochondr	29	1.226902215
5431	P30876	POLR2B	DNA-directed RNA polymerase II sub	36	1.32464413
54332	Q8TB36	GDAP1	Ganglioside-induced differentiation-	1	1.482998613
54431	Q8IXB1	DNAJC10	DnaJ homolog subfamily C member	14	1.373810413
54502	A0AV96	RBM47	RNA-binding protein 47	1	1.546764827
5478	P62937	PPIA	Peptidyl-prolyl cis-trans isomerase A	131	1.475338548
54788	Q9NXW2	DNAJB12	DnaJ homolog subfamily B member	3	1.192257066
54882	Q8IWZ3	ANKHD1	Ankyrin repeat and KH domain-cont	8	1.103012608
54888	Q08J23	NSUN2	tRNA (cytosine(34)-C(5))-methyltran	35	1.39868487
54890	Q6P6C2	ALKBH5	RNA demethylase ALKBH5	4	2.565948517
54948	Q9NX20	MRPL16	39S ribosomal protein L16, mitochon	2	1.435785248
5500	P62140	PPP1CB	Serine/threonine-protein phosphata	72	1.123027052
5511	Q12972	PPP1R8	Nuclear inhibitor of protein phospha	3	1.877904166
55149	Q9NVV4	MTPAP	Poly(A) RNA polymerase, mitochond	6	1.300392161
55160	Q9HCE6	ARHGEF10L	Rho guanine nucleotide exchange fa	2	1.660718583
55161	P57088	TMEM33	Transmembrane protein 33	16	1.15796861
5518	P30153	PPP2R1A	Serine/threonine-protein phosphata	84	1.349852455
55269	Q8WXF1	PSPC1	Paraspeckle component 1	42	2.106950607
552900	Q9H3K6	BOLA2	BolA-like protein 2	36	2.022786416
55602	Q9NXV6	CDKN2AIP	CDKN2A-interacting protein	6	1.600667618
5562	Q13131	PRKAA1	5-AMP-activated protein kinase cata	0	1.432998838
55621	Q9NXH9	TRMT1	tRNA (guanine(26)-N(2))-dimethyltra	11	1.069463929
55644	Q9NPF4	OSGEP	Probable tRNA N6-adenosine threor	4	1.651455514

55651	P55769	NHP2L1	NHP2-like protein 1;NHP2-like prote	36	1.200063837
55699	Q9NSE4	IARS2	Isoleucine--tRNA ligase, mitochondr	6	1.780036076
55720	Q2NL82	TSR1	Pre-rRNA-processing protein TSR1 h	24	2.012986977
55735	Q9NVH1	DNAJC11	DnaJ homolog subfamily C member	5	1.697238115
55750	Q53H12	AGK	Acylglycerol kinase, mitochondrial	13	1.319877698
55754	Q9NV96	TMEM30A	Cell cycle control protein 50A	2	1.606870923
55854	Q8WU90	ZC3H15	Zinc finger CCCH domain-containing	13	1.726400617
5594	P28482	MAPK1	Mitogen-activated protein kinase 1	10	1.190869188
55967	Q9UI09	NDUFA12	NADH dehydrogenase [ubiquinone]	0	1.024009329
5609	O14733	MAP2K7	Dual specificity mitogen-activated p	0	1.688101632
5610	P19525	EIF2AK2	Interferon-induced, double-strande	11	1.031853787
5611	Q13217	DNAJC3	DnaJ homolog subfamily C member	0	1.596322777
56902	Q9NRX1	PNO1	RNA-binding protein PNO1	9	1.867007136
57003	Q96A33	CCDC47	Coiled-coil domain-containing prote	11	1.058637552
5710	P55036	PSMD4	26S proteasome non-ATPase regula	30	1.466368298
57128	Q9HD34	LYRM4	LYR motif-containing protein 4	1	1.219573934
57410	Q96KG9	SCYL1	N-terminal kinase-like protein	2	1.099239806
57414	Q6NTF9	RHBDD2	Rhomboid domain-containing prote	0	1.290094773
57470	Q8N1G4	LRRC47	Leucine-rich repeat-containing prot	22	1.170780207
57532	Q7Z417	NUFIP2	Nuclear fragile X mental retardation	54	1.231585772
57535	Q6UXG2	KIAA1324	UPF0577 protein KIAA1324	1	1.145962275
57665	Q9HBH5	RDH14	Retinol dehydrogenase 14	0	1.445405183
57680	Q9HCK8	CHD8	Chromodomain-helicase-DNA-bindi	6	1.440169035
5825	P28288	ABCD3	ATP-binding cassette sub-family D m	18	1.194634961
58472	Q9Y6N5	SQRDL	Sulfide:quinone oxidoreductase, mit	1	1.299226503
58517	P49756	RBM25	RNA-binding protein 25	38	2.017202935
5868	P20339	RAB5A	Ras-related protein Rab-5A	22	1.609781467
5872	P51153	RAB13	Ras-related protein Rab-13	12	1.727211939
5901	P62826	RAN	GTP-binding nuclear protein Ran	90	1.056246959
59338	Q9HB21	PLEKHA1	Pleckstrin homology domain-contai	0	1.510826779
5976	Q92900	UPF1	Regulator of nonsense transcripts 1	28	1.253928251
60678	P57772	EEFSEC	Selenocysteine-specific elongation f	4	1.213967094
6122	P39023	RPL3	60S ribosomal protein L3	113	1.25915499
6124	P36578	RPL4	60S ribosomal protein L4	148	1.166546556
6125	P46777	RPL5	60S ribosomal protein L5	108	1.273344043
6128	Q02878	RPL6	60S ribosomal protein L6	124	1.039505605
6129	P18124	RPL7	60S ribosomal protein L7	133	1.168946039
6130	P62424	RPL7A	60S ribosomal protein L7a	147	1.228767131
6132	P62917	RPL8	60S ribosomal protein L8	121	1.114128198
6133	P32969	RPL9	60S ribosomal protein L9	114	1.251507092
6135	P62913	RPL11	60S ribosomal protein L11	148	1.612801934
6136	P30050	RPL12	60S ribosomal protein L12	140	1.95482636
6138	P61313	RPL15	60S ribosomal protein L15	105	1.305727451
6139	P18621	RPL17	60S ribosomal protein L17	133	1.428776475
6142	Q02543	RPL18A	60S ribosomal protein L18a	75	1.286128511
6146	P35268	RPL22	60S ribosomal protein L22	133	1.578036766
6147	P62750	RPL23A	60S ribosomal protein L23a	176	1.403126481
6152	P83731	RPL24	60S ribosomal protein L24	135	1.236884828
6155	P61353	RPL27	60S ribosomal protein L27	121	1.470309549
6156	P62888	RPL30	60S ribosomal protein L30	80	1.689813216
6157	P46776	RPL27A	60S ribosomal protein L27a	142	1.347539702
6158	P46779	RPL28	60S ribosomal protein L28	69	1.753932516
6159	P47914	RPL29	60S ribosomal protein L29	117	1.4324129
6160	P62899	RPL31	60S ribosomal protein L31	125	1.329128501

6161	P62910	RPL32	60S ribosomal protein L32	52	1.713382732
6168	P61513	RPL37A	60S ribosomal protein L37a	73	1.805665475
6169	P63173	RPL38	60S ribosomal protein L38	110	1.074960847
6176	P05386	RPLP1	60S acidic ribosomal protein P1	130	1.84872889
6181	P05387	RPLP2	60S acidic ribosomal protein P2	166	1.497512853
6183	O15235	MRPS12	28S ribosomal protein S12, mitocho	2	3.649517785
6187	P15880	RPS2	40S ribosomal protein S2	143	1.502436661
6188	P23396	RPS3	40S ribosomal protein S3	200	1.092043586
6189	P61247	RPS3A	40S ribosomal protein S3a	141	1.078361189
6191	P62701	RPS4X	40S ribosomal protein S4, X isoform	166	1.037619296
6193	P46782	RPS5	40S ribosomal protein S5;40S riboso	112	1.028630662
6195	Q15418	RPS6KA1	Ribosomal protein S6 kinase alpha-1	3	1.394576951
6201	P62081	RPS7	40S ribosomal protein S7	138	1.006996262
6202	P62241	RPS8	40S ribosomal protein S8	163	1.10275037
6203	P46781	RPS9	40S ribosomal protein S9	114	1.01198434
6205	P62280	RPS11	40S ribosomal protein S11	101	1.856915897
6206	P25398	RPS12	40S ribosomal protein S12	94	1.324913956
6207	P62277	RPS13	40S ribosomal protein S13	120	1.03200766
6208	P62263	RPS14	40S ribosomal protein S14	198	1.06582885
6209	P62841	RPS15	40S ribosomal protein S15	89	1.8899015
6210	P62244	RPS15A	40S ribosomal protein S15a	119	1.260230369
6217	P62249	RPS16	40S ribosomal protein S16	147	1.077377427
6218	P08708	RPS17	40S ribosomal protein S17	119	1.400210973
6222	P62269	RPS18	40S ribosomal protein S18	187	1.555903698
6224	P60866	RPS20	40S ribosomal protein S20	116	1.414247772
6227	P63220	RPS21	40S ribosomal protein S21	64	1.982170212
6228	P62266	RPS23	40S ribosomal protein S23	107	1.268895127
6230	P62851	RPS25	40S ribosomal protein S25	154	1.269990021
6231	P62854	RPS26	40S ribosomal protein S26	102	1.396601566
6232	P42677	RPS27	40S ribosomal protein S27	131	2.207135634
6234	P62857	RPS28	40S ribosomal protein S28	119	1.509495703
6389	P31040	SDHA	Succinate dehydrogenase [ubiquino	22	1.201815989
6421	P23246	SFPQ	Splicing factor, proline- and glutami	133	1.935430189
6428	P84103	SRSF3	Serine/arginine-rich splicing factor 3	135	2.744062022
6447	P05408	SCG5	Neuroendocrine protein 7B2;N-term	0	1.680981323
64759	Q68CZ2	TNS3	Tensin-3	2	3.328529339
64761	Q9H0J9	PARP12	Poly [ADP-ribose] polymerase 12	3	1.214681263
64784	Q6UUV7	CRTC3	CREB-regulated transcription coacti	0	1.027704537
64928	Q6P1L8	MRPL14	39S ribosomal protein L14, mitocho	5	1.405641407
64963	P82912	MRPS11	28S ribosomal protein S11, mitocho	3	1.487422187
64965	P82933	MRPS9	28S ribosomal protein S9, mitochon	11	2.539126641
64975	Q8IXM3	MRPL41	39S ribosomal protein L41, mitocho	10	1.202404886
6500	P63208	SKP1	S-phase kinase-associated protein 1	95	1.236318015
65003	Q9Y3B7	MRPL11	39S ribosomal protein L11, mitocho	5	1.082983182
65263	Q53H96	PYCRL	Pyrroline-5-carboxylate reductase 3	4	1.112751285
6576	P53007	SLC25A1	Tricarboxylate transport protein, mi	32	1.395164688
65993	P82930	MRPS34	28S ribosomal protein S34, mitocho	19	1.080395992
6652	Q00796	SORD	Sorbitol dehydrogenase	6	1.520449587
670	Q86WA6	BPHL	Valacyclovir hydrolase	0	1.085739683
6714	P12931	SRC	Proto-oncogene tyrosine-protein ki	13	2.51062284
6726	P49458	SRP9	Signal recognition particle 9 kDa pro	18	1.76966487
6727	P37108	SRP14	Signal recognition particle 14 kDa p	32	1.76360268
6833	Q09428	ABCC8	ATP-binding cassette sub-family C m	0	1.073614305
6850	P43405	SYK	Tyrosine-protein kinase SYK	0	1.532445379

7001	P32119	PRDX2	Peroxiredoxin-2	140	1.057820929
7019	Q00059	TFAM	Transcription factor A, mitochondria	13	1.159674156
708	Q07021	C1QBP	Complement component 1 Q subco	165	1.454560048
7145	Q9HBL0	TNS1	Tensin-1	2	1.532423622
7150	P11387	TOP1	DNA topoisomerase 1	57	1.315908136
7184	P14625	HSP90B1	Endoplasmin	121	2.183448659
7276	P02766	TTR	Transthyretin	0	1.482948252
7277	P68366	TUBA4A	Tubulin alpha-4A chain	309	1.285094739
7284	P49411	TUFM	Elongation factor Tu, mitochondrial	82	1.176301846
7295	P10599	TXN	Thioredoxin	122	1.224621322
7311	P62987	UBA52	Ubiquitin-60S ribosomal protein L40	202	1.431458656
7317	P22314	UBA1	Ubiquitin-like modifier-activating en	63	2.178588688
7388	P07919	UQCRH	Cytochrome b-c1 complex subunit 6	0	1.687060088
7415	P55072	VCP	Transitional endoplasmic reticulum	115	1.494400259
7531	P62258	YWHAE	14-3-3 protein epsilon	129	1.200064942
7534	P63104	YWHAZ	14-3-3 protein zeta/delta	116	1.284080127
7791	Q15942	ZYX	Zyxin	38	1.200175108
7795	Q9Y316	MEMO1	Protein MEMO1	0	1.03485539
7841	Q13724	MOGS	Mannosyl-oligosaccharide glucosida	7	1.47165138
788	O43772	SLC25A20	Mitochondrial carnitine/acylcarnitin	0	1.585001909
79098	Q9BW04	SARG	Specifically androgen-regulated gen	0	1.857753681
79109	Q9BPZ7	MAPKAP1	Target of rapamycin complex 2 subu	0	1.124871765
7913	P35659	DEK	Protein DEK	23	1.174968516
7916	P48634	PRRC2A	Protein PRRC2A	38	2.036903458
79671	Q86UT6	NLRX1	NLR family member X1	3	1.731114435
79726	Q6PJI9	WDR59	WD repeat-containing protein 59	5	1.114740927
79751	Q9H936	SLC25A22	Mitochondrial glutamate carrier 1	4	1.07831461
7991	Q13454	TUSC3	Tumor suppressor candidate 3	1	2.284568973
80775	Q53S58	TMEM177	Transmembrane protein 177	0	1.300955679
8106	Q86U42	PABPN1	Polyadenylate-binding protein 2	24	1.453379432
81567	Q8NBS9	TXNDC5	Thioredoxin domain-containing prot	15	1.693621738
81627	Q7Z2T5	TRMT1L	TRMT1-like protein	19	1.388206603
81855	Q9BWM7	SFXN3	Sideroflexin-3	4	2.253248664
81892	Q9GZT3	SLIRP	SRA stem-loop-interacting RNA-binc	30	1.500229446
81929	Q96EE3	SEH1L	Nucleoporin SEH1	14	1.145626432
830	P47755	CAPZA2	F-actin-capping protein subunit alph	53	1.27736249
83939	Q9BY44	EIF2A	Eukaryotic translation initiation fact	9	1.659117045
8407	P37802	TAGLN2	Transgelin-2	96	1.820156364
84171	Q96JB6	LOXL4	Lysyl oxidase homolog 4	0	1.021681086
84233	Q9H061	TMEM126A	Transmembrane protein 126A	2	1.782051516
84284	Q9BSD7	NTPCR	Cancer-related nucleoside-triphosph	18	1.178449985
84364	Q8N6H7	ARFGAP2	ADP-ribosylation factor GTPase-activ	0	2.678034177
84419	Q9C002	NMES1	Normal mucosa of esophagus-specif	0	1.501070129
84681	Q9BX68	HINT2	Histidine triad nucleotide-binding pr	1	1.683307638
84749	Q70CQ3	USP30	Ubiquitin carboxyl-terminal hydrola	0	1.116454209
84833	Q96IX5	USMG5	Up-regulated during skeletal muscle	2	1.594883007
84883	Q9BRQ8	AIFM2	Apoptosis-inducing factor 2	0	1.726428923
84932	Q8WUD1	RAB2B	Ras-related protein Rab-2B	6	1.026843983
8508	Q9BPW8	NIPSNAP1	Protein NipSnap homolog 1	7	1.334939533
8525	Q13574	DGKZ	Diacylglycerol kinase zeta	1	1.146881501
8826	P46940	IQGAP1	Ras GTPase-activating-like protein I	56	1.267626082
8879	O95470	SGPL1	Sphingosine-1-phosphate lyase 1	5	1.191469572
8890	Q9UI10	EIF2B4	Translation initiation factor eIF-2B s	10	1.05527214
8894	P20042	EIF2S2	Eukaryotic translation initiation fact	0	1.49004533

8904	Q99829	CPNE1	Copine-1	14	1.13241955
89953	Q9NSK0	KLC4	Kinesin light chain 4	7	1.407730155
9054	Q9Y697	NFS1	Cysteine desulfurase, mitochondrial	2	1.111034829
90580	Q9BSF4	C19orf52	Uncharacterized protein C19orf52	2	1.964187656
9060	O95340	PAPSS2	Bifunctional 3-phosphoadenosine 5-	3	1.18370164
9061	O43252	PAPSS1	Bifunctional 3-phosphoadenosine 5-	2	1.079161883
9066	O43581	SYT7	Synaptotagmin-7	0	1.472187842
9126	Q9UQE7	SMC3	Structural maintenance of chromos	28	1.574550468
91289	Q9BU23	LMF2	Lipase maturation factor 2	1	1.13820601
9261	P49137	MAPKAPK2	MAP kinase-activated protein kinas	6	1.755386734
9276	P35606	COPB2	Coatomer subunit beta	39	1.084945317
92906	Q8WVV9	HNRNPLL	Heterogeneous nuclear ribonucleop	15	1.829377782
9349	P62829	RPL23	60S ribosomal protein L23	178	1.32651048
9352	O43396	TXNL1	Thioredoxin-like protein 1	22	1.119078901
9394	O60243	HS6ST1	Heparan-sulfate 6-O-sulfotransferas	0	1.637756564
94081	Q9H9B4	SFXN1	Sideroflexin-1	17	1.065333535
94097	Q8TD22	SFXN5	Sideroflexin-5	0	1.821707534
9414	Q9UDY2	TJP2	Tight junction protein ZO-2	14	3.156417803
9415	O95864	FADS2	Fatty acid desaturase 2	1	1.012233888
9416	Q9BUQ8	DDX23	Probable ATP-dependent RNA helica	32	1.917299455
9501	Q9UNE2	RPH3AL	Rab effector Noc2	0	1.480951297
9524	Q9NZ01	TECR	Very-long-chain enoyl-CoA reductas	33	1.526592238
9553	O75394	MRPL33	39S ribosomal protein L33, mitocho	0	1.350874526
9588	P30041	PRDX6	Peroxiredoxin-6	96	1.120511122
9690	Q15386	UBE3C	Ubiquitin-protein ligase E3C	3	1.516828899
9692	O15091	KIAA0391	Mitochondrial ribonuclease P protei	0	1.125478376
9926	Q92604	LPGAT1	Acyl-CoA:lysophosphatidylglycerol a	1	1.586176789
998	P60953	CDC42	Cell division control protein 42 hom	37	1.026811187
999	P12830	CDH1	Cadherin-1;E-Cad/CTF1;E-Cad/CTF2;	0	1.47250785
9991	O95758	PTBP3	Polypyrimidine tract-binding protei	20	1.510291811

pvalue_IU_vs_CU	MSMSCount_CU	MSMSCount_IU	Detection_CU	Detection_IU	Intensity_CU
4.96774E-05	15	59	6	6	1559799.26
2.5828E-06	1	18	6	6	835411.1111
1.60866E-07	4	15	4	4	127784.3312
8.61574E-09	134	274	6	6	3641696.634
7.20879E-06	63	139	6	6	1050835.592
0.000349539	17	30	6	6	1767444.184
3.59571E-07	2	17	6	5	1233092.168
0.001115445	33	52	6	6	11092406.21
3.83715E-07	0	10	5	5	136905.3243
2.93945E-09	543	868	6	6	7078219.214
0.00330011	23	80	6	6	913674.333
5.32264E-05	58	113	6	6	3970910.288
0.026126036	7	25	6	6	259274.9569
4.92073E-11	1	93	3	6	232840.9641
0.003532637	2	12	5	6	772156.413
0.017504528	16	39	6	6	475892.1112
0.01082403	11	26	3	6	744117.5549
3.65404E-05	30	93	6	6	1439551.6
0.000106678	6	17	5	6	399155.1253
5.75104E-05	1	11	3	5	1238524.474
0.002629385	5	20	4	5	149088.5595
0.002352294	5	16	1	2	1020421.814
0.000167165	33	68	6	6	1822794.196
4.83169E-13	77	229	6	6	2047393.212
2.57031E-06	46	107	6	6	1667853.884
0.00053774	6	20	5	6	831505.0189
8.48226E-07	116	249	6	6	5067199.546
0.000975677	4	25	6	6	5527709.555
0.002088448	49	65	6	6	6900086.333
2.83512E-05	38	102	6	6	1954663.039
5.32661E-10	20	35	6	6	1697754.217
1.32189E-05	27	47	6	6	2765486.033
3.11065E-07	18	43	6	6	3088235.553
0.002189101	12	28	6	6	1686664.123
9.55019E-06	50	60	6	6	704401.203
3.86658E-05	2	12	5	5	132397.9496
0.040860673	0	10	2	3	449890.0683
3.80381E-06	9	41	5	6	858124.9486
0.00031648	24	60	6	6	1536414.786
0.020787184	4	16	5	6	884018.0709
0.000860658	79	186	6	6	6791920.252
0.001185027	0	11	5	6	743014.2446
0.000294335	4	22	5	5	401654.1213
5.51949E-05	18	48	6	6	3569936.936
0.000134537	1	19	5	5	678264.474
0.000212868	7	23	5	5	4130684.538
0.000597255	5	21	6	6	780263.4714
8.92262E-07	44	66	6	6	5215103.061
5.91127E-05	185	208	6	6	7428587.063
0.001196448	7	18	3	3	472634.4868
0.002327641	67	85	6	6	3769034.226
1.86656E-08	238	451	6	6	7127099.098
0.000165397	14	27	5	5	1786247.111

0.008556462	26	49	6	6	1613788.048
0.009553	35	76	5	6	1092712.378
2.31284E-09	70	160	6	6	1207289.379
0.000344195	16	45	6	6	6230974.356
1.71751E-06	171	248	6	6	3288910.816
4.9857E-06	7	20	3	5	848081.565
1.15068E-11	110	214	6	6	2526269.531
1.92643E-05	17	28	6	6	675509.8099
2.64702E-06	10	32	4	5	1555891.239
7.86555E-05	4	31	5	5	466967.8879
3.54552E-05	16	41	6	6	691693.5802
0.003947382	25	72	4	6	1009299.687
0.01434684	35	45	6	6	2415451.946
2.75041E-08	16	42	6	6	2708324.439
5.11784E-05	92	200	6	6	4022807.161
0.000041726	11	35	6	6	873007.9496
0.000149682	60	127	6	6	1561934.688
0.000282944	19	42	6	6	620462.6099
0.006297987	161	293	6	6	50913531.94
2.79727E-07	128	262	6	6	1784989.516
0.00079298	0	26	2	6	891072.523
4.72307E-05	14	24	6	6	686698.5238
1.21853E-05	152	254	6	6	3587726.948
0.007814233	7	21	4	4	1500013.835
1.73808E-10	79	168	6	6	1749602.65
0.013471502	11	51	6	6	3064322.681
1.64369E-09	333	571	6	6	9382402.17
1.86041E-05	29	54	6	6	1196549.769
0.000160042	85	133	6	6	5692931.007
0.002235554	71	149	6	6	2141512.217
9.54794E-07	62	97	6	6	2722222.017
3.53628E-05	15	46	6	6	945602.8052
5.19879E-10	11	24	6	6	1589767.539
8.51E-08	56	124	6	6	1839688.253
1.84462E-05	8	30	6	6	1033775.267
3.77408E-05	18	53	6	6	265697.9162
8.77561E-07	27	90	6	6	2601524.187
3.50018E-06	90	169	6	6	1597544.048
1.91269E-06	79	135	6	6	3733413.865
6.92452E-05	8	24	5	6	1289565.892
0.008200872	18	28	5	6	681097.9902
0.002152535	39	94	6	6	485306.2396
2.98468E-05	15	30	6	6	533879.6201
2.53164E-05	36	50	6	6	1411487.075
1.78923E-07	38	55	6	6	980934.3211
4.69935E-09	188	426	6	6	3407663.151
5.75002E-08	122	200	6	6	3686257.42
0.000874652	2	20	5	6	693817.438
3.94257E-05	68	117	6	6	1390420.128
8.60588E-05	41	108	6	6	664984.5135
1.79353E-10	118	215	6	6	1059671.485
0.001970683	59	91	6	5	1262639.646
0.001345262	6	20	5	6	649380.0072
0.006460751	0	12	2	6	287917.7145

0.001433181	6	18	6	6	177187.9555
0.000383321	98	158	6	6	6809666.881
6.11918E-08	2	14	6	6	594866.5806
0.018350895	11	24	5	6	1486167.618
0.002084508	47	111	6	6	1687708.645
0.011809271	84	140	6	6	4251195.126
5.84307E-06	27	52	6	6	284465.7149
0.0001447	78	130	6	6	2500524.153
0.001243584	41	145	6	6	968000.8225
4.10046E-05	62	115	6	6	1330047.785
0.019880011	0	13	1	3	80542.22888
2.37652E-05	66	127	6	6	12302015.77
0.022726772	7	21	4	6	1597294.366
0.000635312	29	65	6	6	3031422.889
7.01728E-08	94	187	6	6	1310778.717
2.24257E-05	4	21	6	6	1069818.575
3.1172E-06	74	152	6	6	2148798.821
0.000013916	39	82	6	6	1273986.621
3.07538E-05	2	19	5	6	937335.5201
0.003863437	41	103	6	6	9702349.067
0.000535851	3	35	6	6	2545838.302
0.000279151	23	54	4	5	2922683.515
0.004523333	2	18	2	2	537896.6944
0.03763582	130	164	6	6	7980966.919
0.017154451	88	107	6	6	1254938.472
9.29254E-06	0	32	1	6	173054.2167
3.01939E-05	85	161	6	6	2664568.403
5.0058E-06	1	13	5	5	383350.1569
0.009650834	4	20	6	5	1177771.248
7.14583E-06	31	48	6	6	842805.2796
0.001002671	3	25	6	6	386598.1914
0.002762403	21	41	6	6	830808.252
1.83389E-11	31	57	6	6	2117204.9
0.000302338	7	24	6	6	656798.716
2.05741E-05	125	256	6	6	7570293.699
0.003479999	19	57	6	6	1760870.679
1.26616E-08	198	271	6	6	13780378.35
2.77016E-06	50	157	6	6	1377243.587
3.18298E-10	147	255	6	6	4242973.496
1.07919E-06	391	579	6	6	5023032.323
4.15872E-06	93	175	6	6	2364091.437
6.40358E-08	618	815	6	6	10131676.89
0.004896933	0	27	3	6	113548.6151
3.30622E-07	197	438	6	6	10299112.49
0.0037706	11	29	6	6	1737987.309
2.90891E-05	68	108	6	6	3364907.561
0.002666988	2	13	5	5	646095.2341
0.000277461	1	13	6	5	1427915.424
0.009648723	8	41	5	6	2852708.39
5.56524E-05	99	209	6	6	4269233.025
0.001148265	143	252	6	6	7677031.954
0.000270173	358	635	6	6	6297778.262
0	633	1818	6	6	4648726.143
3.59774E-08	319	563	6	6	3502361.446

8.70859E-12	591	1057	6	6	8835698.137
7.99882E-06	450	682	6	6	10457561.08
0.000882203	111	215	6	6	2159437.77
9.18302E-05	51	69	6	6	1151235.784
3.86358E-14	100	1974	6	6	11215157.25
0.001328395	0	12	6	6	939725.5054
0.001439533	23	36	6	6	2727759.931
3.33149E-06	34	65	6	6	422412.3053
0.002288249	7	19	6	6	1066206.87
0.000544514	432	699	6	6	15428013.24
0.01672258	184	322	6	6	13388899.11
1.25855E-07	59	91	6	6	1975001.93
0.000116994	21	51	6	6	3858398.43
3.97473E-05	84	139	6	6	4456950.256
0.002024799	21	59	6	6	2513744.457
0.001525417	12	27	6	6	991433.3774
3.67593E-07	24	65	6	6	518158.6336
5.86553E-06	3	118	5	6	492123.1187
1.08484E-05	134	156	6	6	5198024.325
0.000932065	0	11	5	6	2120583.227
2.90028E-05	19	52	4	5	2559005.906
6.99983E-09	282	565	6	6	3481827.383
0.000264378	78	236	6	6	2143186.004
0.002948386	12	23	5	6	1151015.249
0.00113206	12	41	6	6	766320.2205
9.64957E-06	21	61	6	6	674743.8126
0.000451211	126	193	6	6	9456536.111
0.000514973	25	44	6	5	2413991.937
4.34664E-08	186	368	6	6	3183525.029
1.69824E-09	49	94	6	6	583677.857
1.48852E-07	117	217	6	6	17852668.79
1.56141E-07	99	203	6	6	2655661.775
3.08731E-10	244	428	6	6	2098987.77
1.4121E-07	383	710	6	6	3403661.629
0.000707138	48	79	6	6	2418338.228
0.004603906	27	76	6	6	13097154.33
3.77945E-06	77	162	6	6	11282205.58
5.31063E-05	48	69	6	6	1478205.721
0.000200479	33	50	6	6	3545439.023
0.00151776	23	53	6	6	2553118.167
1.06772E-08	250	371	6	6	2967894.428
6.96745E-11	63	85	6	6	2612619.814
0.000300396	262	378	6	6	2620398.707
5.63152E-07	141	245	6	6	4563197.046
1.78425E-08	23	55	6	6	4444939.521
1.47127E-05	69	82	6	6	2920689.446
3.44772E-07	30	69	6	6	3515170.518
1.33093E-05	49	113	6	6	2803174.56
0.000791294	16	38	6	6	279933.0948
8.08426E-06	16	40	6	6	1559906.228
0.020795732	3	23	3	5	1141738.538
9.46958E-05	152	241	6	6	8237607.77
0.003995896	2	24	3	5	1424566.581
0.002182592	4	18	6	6	168752.1455

0.000018898	18	50	6	6	954597.1454
6.32645E-07	1	12	5	5	1946870.233
3.44329E-05	212	381	6	6	4639985.487
0.000790351	32	52	6	6	2660290.768
1.21796E-08	560	928	6	6	13481920.78
4.21489E-05	19	30	6	5	1360905.215
0.005161057	18	45	6	6	4698329.973
0.00014247	12	35	6	6	2499689.553
4.93314E-07	142	284	6	6	5505380.408
0.001608629	62	88	6	6	3756642.33
1.14106E-08	244	346	6	6	16766688.34
0.000129025	32	60	6	6	630316.7195
0.000672105	42	71	6	6	2357558.397
4.64025E-05	41	58	6	6	1971524.328
0.000692091	25	61	5	5	1273392.741
0.000512611	12	28	5	6	1399307.777
6.33253E-11	79	172	6	6	1015216.286
0.000334283	3	16	6	6	1791004.712
0.00020131	51	73	6	6	2172246.737
3.08494E-06	129	256	6	6	3036906.502
5.0317E-08	122	229	6	6	3126539.133
4.31179E-06	16	42	6	6	2871281.822
0.007140431	10	33	5	5	487654.0385
4.82897E-05	58	70	6	6	1320018.753
1.16282E-06	135	297	6	6	2879838.152
0.002021987	3	19	3	5	128117.9598
2.23539E-05	1	16	5	5	1416852.952
6.00428E-05	656	999	6	6	4600045.599
1.83529E-05	247	386	6	6	10152413.16
0.000155847	14	61	5	6	1007829.967
5.48169E-09	2961	4543	6	6	57768712.05
1.5314E-09	535	817	6	6	23873855.27
1.93346E-06	13	66	6	6	568077.6763
8.64627E-08	194	366	6	6	6474000.473
5.463E-08	31	79	6	6	1310434.101
4.1399E-06	146	244	6	6	2536970.199
4.88201E-06	172	320	6	6	10328660.66
0.005375235	14	33	6	5	703802.6511
0.029632029	19	36	6	6	388403.7581
8.15905E-10	152	319	6	6	3008814.272
0.008425269	0	13	2	3	421842.0605
0.002677959	7	19	6	6	581241.2797
0.00132246	12	33	6	6	1020495.312
5.29275E-05	18	47	6	6	1927598.721
0.019836004	10	32	6	6	5706678.201
0.00644192	0	13	4	5	420963.5616
3.3862E-08	65	100	6	6	1792635.139
0.000158822	11	25	6	6	3030823.28
1.68786E-07	15	51	6	6	1040058.003
6.17103E-05	30	60	6	6	1757793.129
2.70746E-06	14	26	6	6	653229.5923
0.000051051	23	45	6	6	406235.3665
5.17945E-06	4	20	5	6	3190143.924
2.43148E-07	57	134	6	6	1228643.987

3.74588E-05	37	78	6	6	1022216.764
1.40995E-09	202	495	6	6	2523711.077
0.025045513	2	12	3	3	266325.4848
1.58521E-05	31	72	6	6	2284253.133
9.2625E-07	55	104	6	6	2894761.012
2.75593E-05	33	54	6	6	1097823.246
0.001982235	6	17	2	2	708276.9318
0.000110541	79	159	6	6	2401917.748
0.000328006	81	207	6	6	1509847.617
4.11273E-07	2	12	5	6	506868.5593
0.00010408	27	59	6	6	2248519.405
5.33127E-05	46	121	6	6	3042983.606
9.04039E-06	3	23	6	6	645673.3434
0.002876902	126	185	6	6	1686570.945
6.61453E-06	86	176	6	6	5579447.914
0.006569179	5	16	6	6	814801.7386
4.88847E-08	153	213	6	6	1815623.671
4.15379E-05	0	10	5	6	2836550.696
0.000178106	59	139	6	6	1815174.151
0.003455225	10	20	6	6	569913.4655
0.013597506	1	21	4	6	647724.137
6.2357E-07	125	237	6	6	2709614.714
7.26377E-05	11	35	6	6	429119.6355
1.45676E-05	43	75	6	6	2095022.331
1.64855E-11	456	648	6	6	5876860.458
0.000773234	1	33	5	6	754406.8036
0.000216966	45	71	6	6	2618961.659
0.000788316	39	68	6	6	3286965.8
4.8498E-06	327	490	6	6	9858782.985
7.24442E-06	5	37	6	6	1024554.057
3.02442E-07	88	189	6	6	1093379.992
3.54422E-07	28	86	6	6	1196205.437
0.001518909	73	112	6	6	2360184.272
0.006261563	26	92	6	6	1867370.782
1.05317E-08	148	164	6	6	5521425.616
0.011484861	16	51	6	6	1250614.504
0.000275949	22	32	6	6	2748327.875
0.000105474	34	102	6	6	2379891.661
0.000974304	246	376	6	6	7399791.195
3.54939E-08	374	797	6	6	19379084.9
2.07667E-07	282	440	6	6	20282152.03
1.30383E-06	22	57	6	6	3422878.81
7.05103E-05	28	63	6	6	2336128.432
0.00003648	254	430	6	6	6515213.067
0.003647312	30	60	5	6	912605.5308
1.71798E-07	166	179	6	6	51247126.35
2.08679E-09	320	473	6	6	11318567.08
4.68055E-07	251	311	6	6	9919694.346
0.00084643	71	115	6	6	3857036.382
6.38241E-06	116	143	6	6	6887068.1
9.99901E-07	117	153	6	6	7907682.39
3.99002E-05	102	166	6	6	4398949.261
0.018303516	70	109	6	6	21249395.39
0.000633813	86	137	6	6	35876000.89

1.61294E-05	116	270	6	6	3672213.992
7.23787E-05	124	179	6	6	9968916.459
9.88045E-06	247	402	6	6	4877855.264
1.92583E-08	4	23	6	6	3360192.047
0.000088166	13	34	5	6	1698171.845
0.009182087	0	16	2	6	537858.8938
4.86593E-08	393	680	6	6	14186190.41
3.22392E-08	1307	1741	6	6	25709653.07
2.84308E-07	726	1238	6	6	17961177.73
3.9253E-08	514	649	6	6	17030685.47
6.07978E-07	376	656	6	6	25758927.95
1.73778E-07	57	148	6	6	1643262.986
1.48098E-05	338	540	6	6	31969848.1
4.90259E-05	250	384	6	6	4048862.892
9.63517E-07	408	622	6	6	12091483.36
1.58096E-08	170	378	6	6	6312375.103
0.000173666	78	105	6	6	4133517.748
1.30545E-06	365	692	6	6	13183562.26
0.000149599	223	388	6	6	14366563.08
0.000139913	81	157	6	6	17438682.03
6.81397E-06	428	740	6	6	9275681.397
2.87177E-05	563	806	6	6	10494291.53
9.96264E-09	480	754	6	6	14101373.69
9.11012E-07	566	818	6	6	16214321.11
7.98808E-07	315	547	6	6	13410370.47
0.000209523	7	53	6	6	1532879.641
0.000659062	101	229	6	6	15594486.43
0.019257631	177	307	6	6	15474731.39
0.000646172	36	57	5	6	21528732.44
0.000939431	17	32	5	6	2797351.281
0.002188744	42	52	6	6	5415821.003
8.59139E-06	83	171	6	6	3573894.454
1.2102E-07	173	309	6	6	7103872.646
5.86386E-07	51	88	6	6	11959131.52
5.39312E-05	35	121	6	6	840455.8032
3.10862E-14	3	146	6	6	1385645.658
0.007631117	1	13	6	5	585421.5656
6.16055E-05	17	28	6	6	845238.8544
7.61533E-07	36	57	6	6	741732.0093
0.000705361	0	10	4	4	1596441.494
0.013171646	0	10	2	3	362964.0866
0.000296939	21	38	6	6	217358.8225
0.004808538	26	47	6	6	2188143.343
4.78471E-05	51	115	6	6	2214466.144
0.007412803	59	81	6	6	1267593.031
1.10172E-09	181	296	6	6	6515353.739
6.0019E-06	32	48	6	6	415101.7402
0.001952562	0	10	3	5	235288.6151
0.044126278	7	24	3	4	3044500.919
3.18618E-07	6	47	6	6	417250.769
1.8874E-06	69	115	6	6	4471771.12
2.87637E-05	92	294	6	6	9351452.165
0.007184839	89	110	6	6	1773376.957
0.003757053	11	30	6	6	1277665.685

0.000797824	25	89	6	6	2475475.928
6.21043E-05	89	161	6	6	2334390.363
5.59646E-09	23	56	6	5	5340583.645
9.68789E-08	25	95	6	6	814133.9891
0.000234125	4	18	6	6	526828.7278
1.26406E-09	84	251	6	6	1760199.324
3.04812E-06	274	415	6	6	8031078.52
2.82449E-07	69	97	6	6	9149898.053
0.002251608	267	422	6	6	9512783.948
0.004530857	85	135	6	6	1361935.181
0.006504616	3	13	3	4	2390531.45
0.010240107	3	27	5	6	20274107.78
1.01159E-05	21	38	5	6	9974726.839
0.000904423	2	29	5	6	831247.8033
4.50262E-05	33	51	6	6	6117704.454
7.71613E-05	47	57	6	6	3861370.638
0.019410251	18	45	5	6	800341.5481
0.02647076	13	53	5	6	127331.9225
0.000160691	95	193	6	6	2557905.561
0.00008576	7	43	6	6	2296089.673
0.000341987	12	28	5	5	2519847.99
0.002099949	5	18	6	6	665118.0315
3.16271E-06	28	48	6	6	1121457.377
4.20824E-07	22	93	6	6	2104715.969
8.80266E-06	11	25	6	5	462847.4647
1.75181E-05	4	22	6	6	1084030.396
0.000312887	172	323	6	6	2601218.574
0.001524563	5	26	5	6	832868.905
1.1951E-06	22	36	6	6	1242035.47
0.000213372	38	60	6	6	3707663.128
7.22667E-10	97	206	6	6	2552151.232
0.004668298	10	32	6	6	845427.5429
8.65012E-08	89	181	6	6	3698743.581
6.41893E-06	111	215	6	6	4082620.013
0.001867269	9	38	6	6	1662297.39
3.55513E-07	53	102	6	6	2921753.849
9.18253E-09	90	180	6	6	2207468.741
0.000210768	13	40	6	6	1127518.564
0.001821101	27	65	6	6	1231980.781
4.93156E-08	4	25	6	6	2022806.146
2.82341E-11	244	328	6	6	3442406.503
5.49089E-06	7	47	5	6	913039.218
7.11978E-05	103	121	6	6	22105157.82
4.00312E-05	2	25	5	6	1559958.34
2.02196E-05	16	50	6	6	572360.3277
5.36889E-05	76	150	6	6	6844893.891
1.03082E-05	4	14	6	6	638908.2643
0.000618957	9	25	6	6	1075811.438
3.98479E-07	102	162	6	6	7182114.91
0.000965844	19	45	6	6	2094282.737
1.26275E-09	1270	2124	6	6	9711845.382
1.95352E-06	90	191	6	6	2298576.722
6.64915E-05	94	187	6	6	2186230.86
2.62864E-10	187	370	6	6	2188165.207

2.69375E-05	63	101	6	6	3443674.192
0.000814329	28	49	6	6	1005480.418
0.000202754	17	37	6	6	843527.1507
5.74657E-06	31	50	6	6	1935840.86
8.11054E-07	784	1207	6	6	8494752.11
0.000273968	23	36	6	6	1086606.452
0.009695507	3	16	6	6	509071.9746
8.60664E-07	4	30	6	5	810275.4766
0.01222907	31	41	6	6	2942233.22
0.000219308	14	31	6	6	853201.2985
0.000368387	49	97	6	6	1859689.447
2.55462E-06	55	114	6	6	2272838.7
7.45786E-07	136	266	6	6	12665857.72
0.007271397	29	42	6	6	1773752.039
1.31505E-07	1	11	4	6	1004619.901
5.42098E-05	187	348	6	6	5458712.182
0.000273327	10	35	6	6	619843.3311
2.29082E-09	0	19	2	6	706201.6444
0.017749425	42	54	5	6	968300.3079
0.013000935	1	32	4	6	327463.4144
0.000539756	27	71	6	6	1794837.146
4.69173E-06	81	205	6	6	3663617.697
3.77415E-05	11	22	6	6	917708.2223
0.003214356	17	39	6	6	1116459.419
1.00013E-05	34	57	6	6	1190345.53
0.007439656	2	14	6	6	916126.5392
8.07696E-11	92	133	6	6	4338566.957
0.0171388	39	67	6	6	6948991.61
6.30435E-05	15	41	6	6	2661220.378
8.70922E-05	9	32	5	6	1690065.464

Intensity_IU	deltaMSMS_IU.CU	cyt_DE_up	FINAL.CLASSIFICATION	beta
3211022.101	44	no	Vesicles	yes
1433137.505	17	no	Mitochondria	yes
281830.3712	11	no	Degradation	yes
7235168.294	140	no	Secreted	yes
2326247.696	76	no	Trafficking	yes
4584434.495	13	no	Undefined	yes
3394025.766	15	no	Undefined	yes
17752592.3	19	no	Folding	yes
311492.8938	10	no	Undetermined	yes
13927694.68	325	no	Nuclear	yes
2399593.462	57	no	Nuclear	yes
6667326.31	55	no	Cytoskeleton	yes
310673.4053	18	no	Nuclear	yes
9901539.245	92	no	Degradation	yes
1403575.197	10	no	Undetermined	yes
1635182.818	23	no	Undetermined	yes
1895161.176	15	no	Cytoskeleton	yes
3153964.255	63	no	Degradation	yes
1104845.903	11	no	Nuclear	yes
2211224.515	10	no	Trafficking	yes
335867.9986	15	no	Cytoskeleton	yes
4983433.651	11	yes	Secreted	yes
3395277.971	35	no	Undetermined	yes
5205354.07	152	no	Cytoskeleton	yes
2883867.246	61	no	ER	yes
2476450.477	14	no	Nuclear	yes
10170919.79	133	no	Nuclear	yes
12819034.69	21	no	ER	yes
13809445.62	16	no	Undetermined	yes
3599245.124	64	no	Cytoskeleton	yes
3935456.228	15	no	Vesicles	yes
4577577.813	20	yes	Degradation	yes
6714054.978	25	no	Cytoskeleton	yes
3999774.955	16	no	Undetermined	yes
1387275.764	10	yes	Plasma Membrane	yes
446727.1121	10	no	Trafficking	yes
1366821.802	10	no	Cytoskeleton	yes
2434231.547	32	no	Vesicles	yes
3969400.707	36	no	Undetermined	yes
3211063.049	12	no	Nuclear	yes
13574959.78	107	no	Mitochondria	yes
1282264.656	11	no	Undetermined	yes
1184498.876	18	no	ER	yes
7602817.444	30	no	Nuclear	yes
2209956.576	18	no	Nuclear	yes
6388990.479	16	no	Nuclear	yes
2167877.705	16	no	Degradation	yes
11999329.22	22	no	Golgi	yes
13337145.58	23	no	Secreted	yes
1459943.208	11	no	Mitochondria	yes
7448706.07	18	no	Undetermined	yes
16460651.75	213	no	Undetermined	yes
5426877.85	13	no	Vesicles	yes

3066396.359	23	no	Undetermined	yes
2164301.259	41	no	Folding	yes
3488926.534	90	no	Mitochondria	yes
27606937.98	29	no	Mitochondria	yes
7949599.662	77	no	Mitochondria	yes
1914250.833	13	no	Trafficking	yes
7185300.688	104	no	Mitochondria	yes
2428936.716	11	no	Cytoskeleton	yes
3208034.192	22	yes	Mitochondria	yes
1299586.262	27	no	Undetermined	yes
1323150.265	25	no	Cytoskeleton	yes
3095084.378	47	no	Degradation	yes
3495322.685	10	no	Vesicles	yes
4270745.386	26	no	Mitochondria	yes
9373434.768	108	no	Mitochondria	yes
1408350.465	24	no	Mitochondria	yes
3479725.109	67	no	Nuclear	yes
969812.4391	23	yes	Mitochondria	yes
90411108.3	132	no	Protein synthesis	yes
4178260.443	134	no	Degradation	yes
11529939.6	26	no	Protein synthesis	yes
4125559.564	10	no	Protein synthesis	yes
6708797.783	102	no	Undetermined	yes
3715073.752	14	no	Nuclear	yes
2961678.582	89	no	Mitochondria	yes
5833349.416	40	yes	Undetermined	yes
19310666.46	238	no	Undetermined	yes
2251769.587	25	no	Mitochondria	yes
11545488.35	48	no	Undetermined	yes
4672318.866	78	no	Nuclear	yes
5566000.149	35	no	Mitochondria	yes
3286347.378	31	no	Nuclear	yes
10266715.92	13	no	Nuclear	yes
3747889.664	68	no	Plasma Membrane	yes
2259052.244	22	no	Cytoskeleton	yes
526003.1037	35	no	Mitochondria	yes
5180998.393	63	no	Protein synthesis	yes
3212363.935	79	yes	Trafficking	yes
7155496.266	56	no	Folding	yes
2564212.975	16	yes	Mitochondria	yes
7626634.647	10	no	Plasma Membrane	yes
1488707.605	55	no	Cytoskeleton	yes
1176088.478	15	no	Undetermined	yes
3479037.216	14	no	Undetermined	yes
2468806.016	17	no	ER	yes
7231651.625	238	no	Undetermined	yes
7971742.341	78	no	ERAD	yes
2296611.677	18	no	Plasma Membrane	yes
3101154.117	49	no	Plasma Membrane	yes
1269845.985	67	no	Vesicles	yes
2394515.895	97	no	Vesicles	yes
3132835.973	32	no	Nuclear	yes
1691279.072	14	no	Nuclear	yes
793610.9013	12	no	Stress response	yes

3419732.284	12	yes	Undetermined	yes
15208245.15	60	no	Nuclear	yes
1609095.11	12	no	ER	yes
4440569.323	13	yes	Undetermined	yes
5515441.737	64	no	Mitochondria	yes
8149671.983	56	no	Vesicles	yes
698210.6447	25	no	Golgi	yes
4781098.72	52	no	Mitochondria	yes
2120358.194	104	no	Vesicles	yes
3477420.385	53	yes	Stress response	yes
280925.1271	13	no	Undetermined	yes
22889034.41	61	no	Secreted	yes
2478056.622	14	no	Protein synthesis	yes
7144938.588	36	no	Mitochondria	yes
2549395.4	93	no	Nuclear	yes
2650818.36	17	no	Undetermined	yes
4833603.535	78	no	Metabolism	yes
3139573.466	43	no	Undetermined	yes
1591037.692	17	no	Trafficking	yes
21427498.92	62	no	Undetermined	yes
5298429.234	32	no	Cytoskeleton	yes
4759624.8	31	no	Metabolism	yes
1686477.426	16	no	Undetermined	yes
13481442.08	34	no	Secreted	yes
1898092.462	19	no	Undetermined	yes
33459838.61	32	no	ER	yes
5210558.924	76	no	Mitochondria	yes
956119.6419	12	no	Undefined	yes
2585522.703	16	no	Trafficking	yes
2852053.185	17	no	Nuclear	yes
1429346.39	22	yes	Plasma Membrane	yes
1500236.384	20	no	Vesicles	yes
4352349.415	26	no	Nuclear	yes
1405116.362	17	no	Vesicles	yes
16387873.06	131	no	Undetermined	yes
4259926.625	38	no	Nuclear	yes
40829341.52	73	no	Mitochondria	yes
3114349.903	107	no	Undetermined	yes
8199930.844	108	no	Undetermined	yes
9188289.693	188	no	Mitochondria	yes
5801615.9	82	no	Nuclear	yes
17907054.77	197	no	Mitochondria	yes
1502296.245	27	no	Undefined	yes
21367097.4	241	no	Metabolism	yes
3220881.46	18	no	Nuclear	yes
8878165.222	40	no	Secreted	yes
2249314.736	11	no	Stress response	yes
5011099.711	12	no	Undetermined	yes
6490320.651	33	no	Nuclear	yes
8662864.648	110	no	Undetermined	yes
13987038.34	109	no	Protein synthesis	yes
15838283.39	277	no	Nuclear	yes
16841447.2	1185	no	Folding	yes
7962970.399	244	no	Folding	yes

18636717.66	466	no	Folding	yes
21237947.57	232	no	Mitochondria	yes
4651006.52	104	no	Mitochondria	yes
2544827.435	18	no	Undetermined	yes
163190207.9	1874	no	Secreted	yes
8526020.726	12	no	Undetermined	yes
5725348.017	13	no	Undefined	yes
892975.7613	31	no	Plasma Membrane	yes
1952180.878	12	no	Secreted	yes
50579456.47	267	no	Undetermined	yes
27186417.82	138	no	Trafficking	yes
3666706.672	32	no	Cytoskeleton	yes
5580741.338	30	no	Undetermined	yes
7192464.172	55	no	Protein synthesis	yes
6449955.42	38	no	Nuclear	yes
1913979.94	15	no	Undefined	yes
1031293.151	41	no	Undetermined	yes
3952257.894	115	no	Trafficking	yes
15296428.59	22	no	Trafficking	yes
2346978.624	11	no	Cytoskeleton	yes
5211071.104	33	no	Cytoskeleton	yes
6420194.073	283	no	Mitochondria	yes
5289016.655	158	no	Undetermined	yes
2294116.208	11	no	Nuclear	yes
1434678.808	29	no	Undetermined	yes
1654361.11	40	no	Golgi	yes
16972047.71	67	no	Plasma Membrane	yes
3939902.834	19	no	Mitochondria	yes
6642717.287	182	yes	Cytoskeleton	yes
1400033.3	45	no	Undetermined	yes
33432682.84	100	no	Cytoskeleton	yes
5269325.444	104	no	Plasma Membrane	yes
5256622.759	184	no	Cytoskeleton	yes
7917955.557	327	no	Trafficking	yes
3844524.456	31	no	Mitochondria	yes
24641264.66	49	no	Mitochondria	yes
20852220.91	85	no	Mitochondria	yes
3063012.33	21	no	Stress response	yes
8712941.639	17	no	Mitochondria	yes
5150634.057	30	no	Mitochondria	yes
6827129.106	121	no	Mitochondria	yes
7916949.384	22	no	Stress response	yes
6150807.678	116	no	Mitochondria	yes
10786938.13	104	no	Mitochondria	yes
7620634.141	32	no	Mitochondria	yes
6689552.189	13	no	Mitochondria	yes
6008996.474	39	no	Mitochondria	yes
6479395.572	64	yes	Mitochondria	yes
1266870.876	22	no	Nuclear	yes
2306833.821	24	no	Plasma Membrane	yes
3151453.469	20	no	Nuclear	yes
17474149.55	89	no	Nuclear	yes
3835357.23	22	no	Protein synthesis	yes
538916.3956	14	no	Nuclear	yes

1932964.751	32	no	Undetermined	yes
4023753.274	11	yes	Undetermined	yes
9101604.816	169	yes	Mitochondria	yes
5596624.71	20	no	ER	yes
28397125.28	368	no	Mitochondria	yes
2681147.871	11	no	Degradation	yes
6797466.773	27	no	Protein synthesis	yes
4412215.124	23	no	Undetermined	yes
11386483.2	142	no	Vesicles	yes
7296202.375	26	no	Nuclear	yes
41344639.86	102	no	ER	yes
2436484.88	28	no	Cytoskeleton	yes
4952093.074	29	no	Mitochondria	yes
3672414.357	17	yes	Secreted	yes
2101305.52	36	no	Mitochondria	yes
2762355.522	16	no	Nuclear	yes
2965089.026	93	no	Cytoskeleton	yes
5121574.829	13	no	Trafficking	yes
4806934.353	22	no	Trafficking	yes
9204423.539	127	no	Mitochondria	yes
5615560.443	107	no	Mitochondria	yes
5250663.651	26	no	Mitochondria	yes
1429381.264	23	no	Plasma Membrane	yes
2600921.852	12	no	Vesicles	yes
6269088.259	162	no	Folding	yes
328888.547	16	no	Trafficking	yes
2033189.313	15	no	Mitochondria	yes
9181344.012	343	no	ER	yes
17748840.89	139	no	Mitochondria	yes
3855011.01	47	no	Undefined	yes
99581928.07	1582	no	Metabolism	yes
51252256.22	282	no	Mitochondria	yes
1489184.595	53	no	Nuclear	yes
14046829.14	172	no	Mitochondria	yes
3280508.898	48	no	Folding	yes
7752966.136	98	yes	Undetermined	yes
24029437.13	148	no	Folding	yes
1553474.789	19	no	Folding	yes
621568.5453	17	no	Undetermined	yes
6893488.264	167	no	Nuclear	yes
1947875.057	13	no	Undetermined	yes
2276984.276	12	no	Mitochondria	yes
2108099.082	21	no	Nuclear	yes
3525569.2	29	no	Undetermined	yes
7212878.616	22	no	Mitochondria	yes
1438159.163	13	yes	Golgi	yes
3553848.825	35	no	ER	yes
4724873.91	14	no	Undetermined	yes
3495314.083	36	no	Nuclear	yes
3979917.434	30	no	Nuclear	yes
1698899.874	12	no	Folding	yes
1366530.27	22	no	Degradation	yes
6184255.003	16	no	Plasma Membrane	yes
3793091.236	77	no	Nuclear	yes

1715139.455	41	no	#N/A	yes
6436220.606	293	no	Mitochondria	yes
769957.8653	10	no	Nuclear	yes
5544517.998	41	no	Folding	yes
4224305.26	49	no	Mitochondria	yes
4555861.906	21	no	Mitochondria	yes
2236831.577	11	no	Undetermined	yes
4736321.94	80	no	Stress response	yes
3969215.565	126	no	Stress response	yes
2031592.201	10	no	Plasma Membrane	yes
4812211.047	32	no	Stress response	yes
6714758.11	75	no	Folding	yes
1548323.757	20	no	Nuclear	yes
3176205.251	59	no	ER	yes
8702750.864	90	no	Degradation	yes
2572243.599	11	no	Nuclear	yes
4139259.754	60	no	Trafficking	yes
11989608.88	10	no	Secreted	yes
3891873.799	80	no	Undetermined	yes
1279290.059	10	no	Protein synthesis	yes
880652.8193	20	no	Undetermined	yes
3791370.756	112	no	ER	yes
961825.7827	24	no	Nuclear	yes
3763819.561	32	no	Vesicles	yes
12455841.73	192	yes	Mitochondria	yes
2592177.65	32	no	Nuclear	yes
5540811.528	26	no	Trafficking	yes
5115553.978	29	no	Plasma Membrane	yes
16223751.55	163	no	Nuclear	yes
1900910.073	32	no	Undetermined	yes
2323616.494	101	no	Undetermined	yes
2880941.804	58	no	Nuclear	yes
5060821.05	39	no	Protein synthesis	yes
3686255.1	66	no	Protein synthesis	yes
8873659.533	16	no	Protein synthesis	yes
2588104.519	35	no	Protein synthesis	yes
6338347.322	10	no	ER	yes
4613139.788	68	no	Protein synthesis	yes
14538068.17	130	no	Protein synthesis	yes
40778758.58	423	no	Protein synthesis	yes
40622415.61	158	no	Protein synthesis	yes
7432092.673	35	no	Golgi	yes
4826397.074	35	no	Protein synthesis	yes
15780214.19	176	no	Protein synthesis	yes
1967356.638	30	no	Protein synthesis	yes
116146441.3	13	no	Protein synthesis	yes
29653502.38	153	no	Protein synthesis	yes
21656447.25	60	no	Protein synthesis	yes
10575645.89	44	no	Protein synthesis	yes
10149687.11	27	no	Protein synthesis	yes
19912224.97	36	no	Protein synthesis	yes
9326986.725	64	no	Protein synthesis	yes
48363666.39	39	no	Protein synthesis	yes
71696335.83	51	no	Protein synthesis	yes

7975061.707	154	no	Protein synthesis	yes
19271961.14	55	no	Protein synthesis	yes
10802031.6	155	no	Protein synthesis	yes
8891230.409	19	no	Protein synthesis	yes
3656998.023	21	no	Mitochondria	yes
7671482.568	16	no	Mitochondria	yes
33828687.05	287	no	Protein synthesis	yes
39517196.89	434	no	Protein synthesis	yes
40100564	512	no	Protein synthesis	yes
36816215.23	135	no	Protein synthesis	yes
41476339.13	280	no	Protein synthesis	yes
2981999.414	91	yes	Undefined	yes
60994148.3	202	no	Protein synthesis	yes
6788504.268	134	no	Protein synthesis	yes
25568251.28	214	no	Protein synthesis	yes
16126467.94	208	no	Protein synthesis	yes
5523044.515	27	no	Protein synthesis	yes
31502441.48	327	no	Protein synthesis	yes
30003687.39	165	no	Protein synthesis	yes
33793017.3	76	no	Protein synthesis	yes
17055421.21	312	no	Protein synthesis	yes
25063256.15	243	no	Protein synthesis	yes
28788011.49	274	no	Protein synthesis	yes
32350841.15	252	no	Protein synthesis	yes
23130890.8	232	no	Protein synthesis	yes
2649722.676	46	no	Protein synthesis	yes
34858454.96	128	no	Protein synthesis	yes
32216901.51	130	no	Protein synthesis	yes
49812601.91	21	no	Protein synthesis	yes
7394536.471	15	no	Protein synthesis	yes
18279862.35	10	no	Protein synthesis	yes
6602169.414	88	no	Mitochondria	yes
13586824.95	136	no	Nuclear	yes
28165465.86	37	no	Protein synthesis	yes
1870329.934	86	no	Secreted	yes
4482877.02	143	no	Undetermined	yes
839022.6905	12	no	Undefined	yes
1614151.806	11	no	Nuclear	yes
1983870.686	21	yes	Mitochondria	yes
4135293.508	10	no	Protein synthesis	yes
1947795.514	10	no	Mitochondria	yes
755156.7536	17	no	Protein synthesis	yes
3191050.803	21	no	Degradation	yes
4360921.531	64	no	Mitochondria	yes
1972960.299	22	no	Nuclear	yes
13487366.93	115	no	Mitochondria	yes
1346460.403	16	no	Mitochondria	yes
693540.5049	10	no	Undetermined	yes
5200121.373	17	no	Undetermined	yes
2848991.075	41	yes	ER	yes
13161516.13	46	no	Undefined	yes
20528042.66	202	no	Protein synthesis	yes
3588272.559	21	no	Plasma Membrane	yes
1948255.508	19	no	Undetermined	yes

9096323.779	64	no	Stress response	yes
5657113.968	72	no	Mitochondria	yes
8363790.617	33	no	Plasma Membrane	yes
2291240.915	70	yes	Plasma Membrane	yes
1054941.401	14	no	Undefined	yes
4679310.553	167	no	Folding	yes
16712952.21	141	no	Golgi	yes
15658988.19	28	no	Cytoskeleton	yes
15368488.52	155	no	Mitochondria	yes
2983438.229	50	yes	Folding	yes
8711061.168	10	no	Protein synthesis	yes
46841808.13	24	no	Degradation	yes
18529169.92	17	no	Mitochondria	yes
6629043.547	27	no	ERAD	yes
10894738.49	18	no	Mitochondria	yes
6700133.142	10	no	Undetermined	yes
3276782.813	27	yes	Undetermined	yes
276194.0407	40	no	#N/A	yes
5665508.177	98	no	Metabolism	yes
3771012.419	36	no	Mitochondria	yes
3519510.097	16	no	Undetermined	yes
2063782.13	13	no	Undetermined	yes
1565230.739	20	no	Nuclear	yes
4516393.251	71	no	Undetermined	yes
11327991.06	14	no	Mitochondria	yes
3195081.871	18	no	Undetermined	yes
5878952.763	151	yes	Mitochondria	yes
1724624.698	21	no	ER	yes
2881023.487	14	no	Undetermined	yes
7846687.234	22	no	Nuclear	yes
5571806.696	109	no	Folding	yes
2220906.512	22	no	Nuclear	yes
6330569.537	92	no	Mitochondria	yes
9518450.878	104	no	Mitochondria	yes
3846509.938	29	no	Undetermined	yes
5574859.564	49	no	ER	yes
5154269.919	90	no	Stress response	yes
5711800.771	27	no	Cytoskeleton	yes
1784084.214	38	no	Secreted	yes
5476199.749	21	no	Mitochondria	yes
6405775.137	84	no	Undefined	yes
3983976.6	40	no	Trafficking	yes
60386843.61	18	no	Nuclear	yes
3101449.883	23	no	Mitochondria	yes
1762610.252	34	no	Degradation	yes
15785405.53	74	no	Mitochondria	yes
1771487.792	10	yes	Mitochondria	yes
1837574.279	16	no	Undetermined	yes
12337669.87	60	no	Degradation	yes
2384817.478	26	no	Undefined	yes
20247166.58	854	no	Cytoskeleton	yes
5827427.141	101	no	ER	yes
3150121.956	93	no	Protein synthesis	yes
4563037.186	183	no	ER	yes

7498773.981	38	no	Vesicles	yes
2263790.02	21	no	Trafficking	yes
2402486.255	20	no	Undefined	yes
6568478.958	19	no	#N/A	yes
13945623.17	423	yes	Mitochondria	yes
2847298.638	13	no	Nuclear	yes
1956651.629	13	no	Trafficking	yes
2306388.075	26	no	Secreted	yes
6832066.208	10	no	Undetermined	yes
2451106.121	17	no	Undefined	yes
3706535.628	48	no	Trafficking	yes
4769372.447	59	no	Undetermined	yes
26768225.08	130	no	Protein synthesis	yes
3797025.108	13	no	Undetermined	yes
3409826.709	10	no	Golgi	yes
9736177.606	161	no	Mitochondria	yes
2036772.659	25	no	Mitochondria	yes
1591722.429	19	no	Plasma Membrane	yes
2024021.749	12	no	Undetermined	yes
32190492.45	31	no	Nuclear	yes
3709354.942	44	no	Undetermined	yes
5532596.813	124	no	ER	yes
2894070.772	11	no	Mitochondria	yes
1718209.457	22	no	Metabolism	yes
3098695.273	23	no	Degradation	yes
1235616.566	12	no	Mitochondria	yes
9612953.796	41	yes	ER	yes
14615050.72	28	no	Plasma Membrane	yes
6943225.35	26	no	Plasma Membrane	yes
3273343.321	23	no	Nuclear	yes

Supplementary Table 3 - ER folding factors in Proinsulin interactome

	Description
IU	Normal Human Islets immunoprecipitated by proinsulin specific antibody 20G11-conju
CU	Normal Human Islets control immunoprecipitation by mouse IgG-conjugated beads
beta	Confirmed expression in single cell RNA-seq data (Ref 22)

ugated beads

EID	Protein	Genenames	Proteinnames	foundExp_C	log2FC_IU_
10549	Q13162	PRDX4	Peroxiredoxin-4	101	6.1718535
23071	Q9BS26	ERP44	Endoplasmic reticulum resident protein 44	10	1.585073
23197	Q96CS3	FAF2	FAS-associated factor 2	6	1.3770459
3309	P11021	HSPA5	78 kDa glucose-regulated protein	292	2.5934031
3312	P11142	HSPA8	Heat shock cognate 71 kDa protein	328	1.5706375
5034	P07237	P4HB	Protein disulfide-isomerase	72	0.9789825
50506	Q9NRD8	DUOX2	Dual oxidase 2	0	1.6990004
51726	Q9UBS4	DNAJB11	DnaJ homolog subfamily B member 11	27	1.9097846
54431	Q8IXB1	DNAJC10	DnaJ homolog subfamily C member 10	14	1.3738104
54788	Q9NXW2	DNAJB12	DnaJ homolog subfamily B member 12	3	1.1922571
5611	Q13217	DNAJC3	DnaJ homolog subfamily C member 3	0	1.5963228
56605	Q86YB8	ERO1LB	ERO1-like protein beta	1	0.9959675
5768	O00391	QSOX1	Sulfhydryl oxidase 1	1	1.0143336
7184	P14625	HSP90B1	Endoplasmin	121	2.1834487
7295	P10599	TXN	Thioredoxin	122	1.2246213
7415	P55072	VCP	Transitional endoplasmic reticulum ATPase	115	1.4944003
81567	Q8NBS9	TXNDC5	Thioredoxin domain-containing protein 5	15	1.6936217
9352	O43396	TXNL1	Thioredoxin-like protein 1	22	1.1190789

pvalue_IU_	MSMSCoun	MSMSCoun	Detection_	Detection_I	Intensity_C	Intensity_IU	deltaMSMS	cyt_DE_up
4.92E-11	1	93	3	6	232840.96	9901539.2	92	no
1.91E-06	79	135	6	6	3733413.9	7155496.3	56	no
5.75E-08	122	200	6	6	3686257.4	7971742.3	78	no
0	633	1818	6	6	4648726.1	16841447	1185	no
3.60E-08	319	563	6	6	3502361.4	7962970.4	244	no
3.33E-04	16	31	6	6	2576408.5	4859864.9	15	no
6.33E-07	1	12	5	5	1946870.2	4023753.3	11	yes
1.16E-06	135	297	6	6	2879838.2	6269088.3	162	no
5.46E-08	31	79	6	6	1310434.1	3280508.9	48	no
0.0053752	14	33	6	5	703802.65	1553474.8	19	no
5.33E-05	46	121	6	6	3042983.6	6714758.1	75	no
9.91E-04	11	18	6	6	2517169.6	4706669.2	7	no
0.0466975	2	6	5	6	1633169.9	2458173.6	4	yes
1.26E-09	84	251	6	6	1760199.3	4679310.6	167	no
0.0045309	85	135	6	6	1361935.2	2983438.2	50	yes
9.04E-04	2	29	5	6	831247.8	6629043.5	27	no
7.23E-10	97	206	6	6	2552151.2	5571806.7	109	no
0.0072714	29	42	6	6	1773752	3797025.1	13	no

FINAL.CLAS	**beta**	**family.label**
Degradatior	yes	Oxidoreductase
Folding	yes	Oxidoreductase
ERAD	yes	ERAD
Folding	yes	Chaperones
Folding	yes	Chaperones
Folding	yes	Oxidoreductase
Undetermir	yes	Oxidoreductase
Folding	yes	Cochaperones
Folding	yes	Cochaperones
Folding	yes	Cochaperones
Folding	yes	Cochaperones
ER	yes	Oxidoreductase
Trafficking	yes	Oxidoreductase
Folding	yes	Chaperones
Folding	yes	Oxidoreductase
ERAD	yes	ERAD
Folding	yes	Oxidoreductase
Undetermir	yes	Oxidoreductase

Checklist for Reporting Human Islet Preparations Used in Research

Adapted from Hart NJ, Powers AC (2018) Progress, challenges, and suggestions for using human islets to understand islet biology and human diabetes. Diabetologia https://doi.org/10.1007/s00125-018-4772-2.

Manuscript DOI: https://doi.org/10.2337/DB20-0245 **(**Example, https://doi.org/10.2337/db18-1234)	
Title: Unbiased profiling of the human proinsulin biosynthetic interaction network reveals a role for peroxiredoxin 4 in proinsulin folding	
Author list: Duc T. Tran, Anita Pottekat, Saiful A. Mir, Insook Jang, Salvatore Loguercio, Alexandre Rosa Campos, Kathleen M. Scully, Reyhaneh Lahmy, Ming Liu, Peter Arvan, William E. Balch, Randal J. Kaufman, Pamela Itkin-Ansari	
Corresponding author: Pamela Itkin-Ansari	**Email address:** pitkin@sbpdiscovery.org

Islet preparation	1	2	3	4	5	6	7	8[a]
MANDATORY INFORMATION								
Unique identifier	HP-18047-01	HP-18087-01	HP-19113-01	RRID:SAMN11633049	HP-18038-01T2D	HP-18068-01T2D	HP-18103-01T2D	RRID:SAMN11642375
Donor age (years)	28	58	35	48	35	55	45	58

Donor sex (M/F)	M	M	F	M	F	M	M	M
Donor BMI (kg/m^2)	34.32	31.8	33.3	38.75	34.0	29.9	27.3	32.5
Donor HbA$_{1c}$ or other measure of blood glucose control	4.2%	5.9%	5.4%	Blood glucose 149.4 mg/dL	7.1%	8.5%	6.5%	6.7%
Origin/source of islets[b]	Prodo Labs	Prodo Labs	Prodo Labs	Integrated Islet Distribution program	Prodo Labs	Prodo Labs	Prodo Labs	Integrated Islet Distribution program
Islet isolation centre	Prodo Labs	Prodo Labs	Prodo Labs	Integrated Islet Distribution program	Prodo Labs	Prodo Labs	Prodo Labs	Integrated Islet Distribution program
Donor history of diabetes? Yes/No	No	No	No	No	Yes	Yes	Yes	Yes
If Yes, complete the next two lines if this information is available								
Diabetes duration (years)					0.5	3.0		0-5
Glucose-lowering therapy at time of death[c]					Managing with diet	Metformin	Managing with diet	Diet, insulin therapy

RECOMMENDED INFORMATION

Donor cause of death	Head trauma	stroke	stroke	stroke	stroke	Head trauma	stroke	stroke
Warm ischaemia time (h)								
Cold ischaemia time (h)								
Estimated purity (%)	95	90	98	90	85	85	85-90	85
Estimated viability (%)	95	95	95	98	95	95	95	95
Total culture time (h)[d]								
Glucose-stimulated insulin secretion or other functional measurement[e]								
Handpicked to purity? Yes/No	No	No	No	No	No	No		No
Additional notes								

[a] If you have used more than eight islet preparations, please complete additional forms as necessary

[b] For example, IIDP, ECIT, Alberta IsletCore

[c] Please specify the therapy/therapies

[d] Time of islet culture at the isolation centre, during shipment and at the receiving laboratory

[e] Please specify the test and the results

American Diabetes Association. diabetes

Checklist for Reporting Human Islet Preparations Used in Research

Adapted from Hart NJ, Powers AC (2018) Progress, challenges, and suggestions for using human islets to understand islet biology and human diabetes. Diabetologia https://doi.org/10.1007/s00125-018-4772-2.

Manuscript DOI: https://doi.org/10.2337/DB20-0245 **(**Example, https://doi.org/10.2337/db18-1234)	
Title: Unbiased profiling of the human proinsulin biosynthetic interaction network reveals a role for peroxiredoxin 4 in proinsulin folding	
Author list: Duc T. Tran, Anita Pottekat, Saiful A. Mir, Insook Jang, Salvatore Loguercio, Alexandre Rosa Campos, Kathleen M. Scully, Reyhaneh Lahmy, Ming Liu, Peter Arvan, William E. Balch, Randal J. Kaufman, Pamela Itkin-Ansari	
Corresponding author: Pamela Itkin-Ansari	**Email address:** pitkin@sbpdiscovery.org

Islet preparation	1	2	3	4	5	6	7	8[a]
MANDATORY INFORMATION								
Unique identifier	HP-16020-01	HP-16007-01	HP-15338-01	HP-15315-01	HP-15259-01	HP-15232-01	HP-15157-01	HP-19038-01
Donor age (years)	57	56	41	51	37	36	27	55

Donor sex (M/F)	F	F	M	F	M	F	M	M
Donor BMI (kg/m^2)	23.1	23.1	24.6	21.0	25.4	24.6	18.3	28.1
Donor HbA_{1c} or other measure of blood glucose control	5.0%	5.4%	5.4%	5.3%	5.5%	4.8%	5.8%	5.0%
Origin/source of islets[b]	Prodo Labs	Prodo Labs	Prodo Labs	Prodo Labs	Prodo Labs	Prodo Labs	Prodo Labs	Prodo Labs
Islet isolation centre	Prodo Labs	Prodo Labs	Prodo Labs	Prodo Labs	Prodo Labs	Prodo Labs	Prodo Labs	Prodo Labs
Donor history of diabetes? Yes/No	No	No	No	No	No	No	No	No
If Yes, complete the next two lines if this information is available								
Diabetes duration (years)								
Glucose-lowering therapy at time of death[c]								

RECOMMENDED INFORMATION								
Donor cause of death	stroke	stroke	stroke	stroke	stroke	stroke	Head trauma	stroke

Warm ischaemia time (h)								
Cold ischaemia time (h)								
Estimated purity (%)								
Estimated viability (%)								
Total culture time (h)[d]								
Glucose-stimulated insulin secretion or other functional measurement[e]								
Handpicked to purity? Yes/No								
Additional notes								

[a] If you have used more than eight islet preparations, please complete additional forms as necessary

[b] For example, IIDP, ECIT, Alberta IsletCore

[c] Please specify the therapy/therapies

[d] Time of islet culture at the isolation centre, during shipment and at the receiving laboratory

[e] Please specify the test and the results

Checklist for Reporting Human Islet Preparations Used in Research

Adapted from Hart NJ, Powers AC (2018) Progress, challenges, and suggestions for using human islets to understand islet biology and human diabetes. Diabetologia https://doi.org/10.1007/s00125-018-4772-2.

Manuscript DOI: https://doi.org/10.2337/DB20-0245 (Example, https://doi.org/10.2337/db18-1234)	
Title: Unbiased profiling of the human proinsulin biosynthetic interaction network reveals a role for peroxiredoxin 4 in proinsulin folding	
Author list: Duc T. Tran, Anita Pottekat, Saiful A. Mir, Insook Jang, Salvatore Loguercio, Alexandre Rosa Campos, Kathleen M. Scully, Reyhaneh Lahmy, Ming Liu, Peter Arvan, William E. Balch, Randal J. Kaufman, Pamela Itkin-Ansari	
Corresponding author: Pamela Itkin-Ansari	**Email address:** pitkin@sbpdiscovery.org

Islet preparation	1	2	3	4	5	6	7	8[a]
MANDATORY INFORMATION								
Unique identifier	HP-19324-01							
Donor age (years)	43							

Donor sex (M/F)	F							
Donor BMI (kg/m^2)	22.8							
Donor HbA$_{1c}$ or other measure of blood glucose control	5.4%							
Origin/source of islets[b]	Prodo Labs							
Islet isolation centre	Prodo Labs							
Donor history of diabetes? Yes/No	No							
If Yes, complete the next two lines if this information is available								
Diabetes duration (years)								
Glucose-lowering therapy at time of death[c]								

RECOMMENDED INFORMATION								
Donor cause of death	stroke							

Warm ischaemia time (h)								
Cold ischaemia time (h)								
Estimated purity (%)	95							
Estimated viability (%)	95							
Total culture time (h)[d]								
Glucose-stimulated insulin secretion or other functional measurement[e]								
Handpicked to purity? Yes/No	No							
Additional notes								

[a] If you have used more than eight islet preparations, please complete additional forms as necessary

[b] For example, IIDP, ECIT, Alberta IsletCore

[c] Please specify the therapy/therapies

[d] Time of islet culture at the isolation centre, during shipment and at the receiving laboratory

[e] Please specify the test and the results